Otpornost betonskog elementa izloženog djelovanju povišene temperature : 3D studija konačnim elementima

Jukić, Martina

SVEUČILIŠTE U SPLITU
FAKULTET GRAĐEVINARSTVA ARHITEKTURE I GEODEZIJE

DIPLOMSKI RAD

Martina Jukić

Split, 2019.

SVEUČILIŠTE U SPLITU
FAKULTET GRAĐEVINARSTVA, ARHITEKTURE I GEODEZIJE

Martina Jukić

Otpornost betonskog elementa izloženog djelovanju povišene temperature: 3D studija konačnim elementima

Diplomski rad

Split, 2019.

Otpornost betonskog elementa izloženog djelovanju povišene temperature: 3D studija konačnim elementima

Sažetak:

Tema diplomskog rada bila je istražiti utjecaj povišenog djelovanja temperature na nosivost i oštećenje betona betonskog elementa u kojem je prethodno ugrađeno sidro blizu ruba elementa. Promatrani su slučajevi bez prethodnog opterećenja silom okomito na rub elementa i sa prethodnim opterećenjem silom okomito na rub. Također su promatrani slučajevi opterećivanja do sloma neposredno nakon djelovanja visoke temperature te nakon potpunog hlađenja elementa.

Napravljeno je više modela ovisno o efektivnoj duljini sidra, udaljenosi osi sidra od ruba betonskog elementa i promjeru sidra. Prikazani su proračuni i rezultati te parametrska studija pri kojoj su se mijenjale različite duljine vremena djelovanja požara.

Ključne riječi:

Betonski element, sidro, pukotine, opterećenje, oštećenje betona, visoka temperatura

Concrete edge failure of headed stud anchor after fire exposure: 3D finite element study

Abstract:

The topic of the thesis was to investigate the impact of elevated temperature action on the loading capacity and damage of concrete on a concrete elementwith an anchor installed near the edge. Calculation was made for cases without pre-loading and for cases with pre-loading. The loading process of the concrete element up to failure was made for two cases. First one is loading immediately after high temperature action and the other one is loading after the complete cooling of the element.

Models were made in dependance of effective lenght of anchors, distance between the anchor and the edge of the element and the diameter of the anchor. The calculations and results are shown for different duration of fire time.

Keywords:

Concrete element, anchor, cracks, load, damage of concrete, high temperatures

SVEUČILIŠTE U SPLITU
FAKULTET GRAĐEVINARSTVA, ARHITEKTURE I GEODEZIJE

STUDIJ:	**DIPLOMSKI SVEUČILIŠNI STUDIJ GRAĐEVINARSTVA**
KANDIDAT:	MARTINA JUKIĆ
BROJ INDEKSA:	694
KATEDRA:	**Katedra za betonske konstrukcije i mostove**
PREDMET:	Betonske konstrukcije II

ZADATAK ZA DIPLOMSKI RAD

Tema: Otpornost betonskog elementa izloženog djelovanju povišene temperature: 3D studija konačnim elemenatima

Opis zadatka: Potrebno je izvršiti analizu betonskog elementa izloženog djelovanju požara

U Splitu, 06.09.2019.

Voditelj Diplomskog rada:

Prof.dr.sc. Alen Harapin

Komentor:

Prof.dr.sc. Joško Ožbolt

Predsjednik Povjerenstva

za završne i diplomske ispite:

Doc. dr. sc. Ivo Andrić

Ovaj diplomski rad je izrađen na Institutu za građevinske materijale, Sveučilište u Stuttgartu

UNIVERSITY OF STUTTGART
Institut für Werkstoffe im Bauwesen
70560 Stuttgart
Germany

Concrete edge failure of headed stud anchor after fire exposure: 3D finite element study

Dissertation submitted for the degree of Master of Civil Engineering in Structures

Author

Martina Jukić

Supervisor

prof.dr.sc. Joško Ožbolt

Stuttgart, July, 2019.

Table of Contents

1. INTRODUCTION

1.1 General task

Fire is a phenomenon of fiery inflammation, unwanted and not controlled by people. It occurs in unpredictable locations and is caused by a completely random contribution of energy. Because of its unpredictable effect, it is one of the deadliest and most dangerous disasters, whether natural or caused by human activity. Fire can be caused by collision, transportation of flammable material, leakage of gas, electrical malfunction, earthquake, and so on.

Concrete, as the most widely used man made material, is recognized as a good fireproof material. Due to low thermal conductivity, the concrete structure is relatively safe from the fire. It can whitstand longer fire durations than steel structure. However, numerous studies have revealed that concrete exhibits the degradation of mechanical properties and even surface spalling under the influence of fire, enpecially high strength concrete. Therefore, a fire engineer should pay close attention to local surface spalling or cracking of concrete that can expose the reinforcement to high temperature and thus endanger the whole structure rapidly.

Anchorages in concrete are widely used in structures for connecting various components. Building fire disaster commonly starts with the burning and falling of the claddings and attachments fastened to the main concrete structure, which has been the case in many recorded fire accidents. The destruction of claddings or curtain wall usually facilitates the spread of fire to adjacent spaces and also accelerates the fire damage of the main structure.

Numerous investigations on concrete failure of anchors at ambient temperature exist so far. However, the load-bearing behaviour at elevated temperatures, such as fire, has barely been investigated. Due to the softening of steel at high temperature in case of fire, steel failure might be the governing failure mode. However, even if the steel parts are protected against fire or specially designed, a single fastener or a group of fasteners close to edge of concrete member or shallowly embedded in concrete may fail from concrete breakout because the concrete material starts to exhibit rapid reduction in mechanical properties under fire exposure, especially after cooling.

1.2 Overview of the work

The main objective of this thesis is to investigate the load-bearing behaviour of headed stud anchor in concrete, loaded in shear after fire exposure due to concrete failure. The concrete edge failure resistance of anchor is studied in the hot state (immediately after heating) and in the cold state (after cooling of the concrete specimen). Different anchorage configurations and parameters like concrete edge distance, embedment depth, stud diameter and fire duration are considered.

1.3 General about computer programs MASA i Femap®

"Finite element program MASA (Macroscopic Space Analysis) is aimed to be applied for nonlinear three-dimensional (3D) analysis of structures made of quasi-brittle materials, such as concrete, stones, ceramics and similar materials. Although different kind of materials can be analyzed, the program is mainly intended for the nonlinear analysis of concrete and reinforced concrete (RC) structures. Theoretical background is continuum mechanics and irreversible thermodynamics. The program can be used for solving mechanical problems, such as static and dynamic analysis of structures, non-mechanical problems, such as analysis of transport processes in porous media, and for the study of coupled problems, such as analysis of concrete at high temperature or analysis of corrosion of reinforcement. To prepare input data as well as to analyze the results of the finite element analysis, commercial pre- and post-processing package FEMAP® is used. It generates nodes, nodal connectivities, boundary conditions, material data and loads, which are required for the finite element analysis. The link between FEMAP® and MASA is realized through an input interface program, which from FEMAP® output data (neutral file) generates input data for the FE code. The interface program can run directly from the MASA main control graphical used interface. Moreover, to generate post-processing output results from the numerical results of the FE code, an output interface program is used. The post-processing output results can be read and graphically interpreted by FEMAP®." [4]

In the past different constitute models and methods were proposed to simulate the mechanical behaviour of concrete: linear- and non-linear fracture mechanics, continuum damage mechanics, plasticity theory, microplane model, and others. Among the various theories describing the mechanical behaviour of concrete, microplane model has proved to be one of the more accurate methods. In this work, the thermomechanical model is based on a temperature-dependent microplane model(Ožbolt et al., 2005b; Ožbolt et al., 2005a).In the microplane model, stresses and strains are

monitored in directions which are previously defined. Based on that, response of material is calculated. It is possible to calculate the macroscopic stress tensor if the macroscopic strain tensor is known due to integration of the microplane stresses and strains.In the microplane model the material is characterized by the relation between stress and strain components on planes of various orientations. These planes can represent the damage planes or weak planes in the microstructure, such as those that exist at the contact between aggregate and cement matrix.(Figure) The used microplane model (Ožbolt et al., 2001) is based on the so-called relaxed kinematic constraint concept. Each microplane is defined by its unit normal vector components n_i (Figure 3.13b). Microplane strains are assumed to be the projections of macroscopic strain tensor 44 ε_{ij} (kinematic constraint). On the microplane normal (σ_N, ε_N) and two shear stress–strain components (σ_K, σ_M, ε_K, ε_M) are considered. [3]

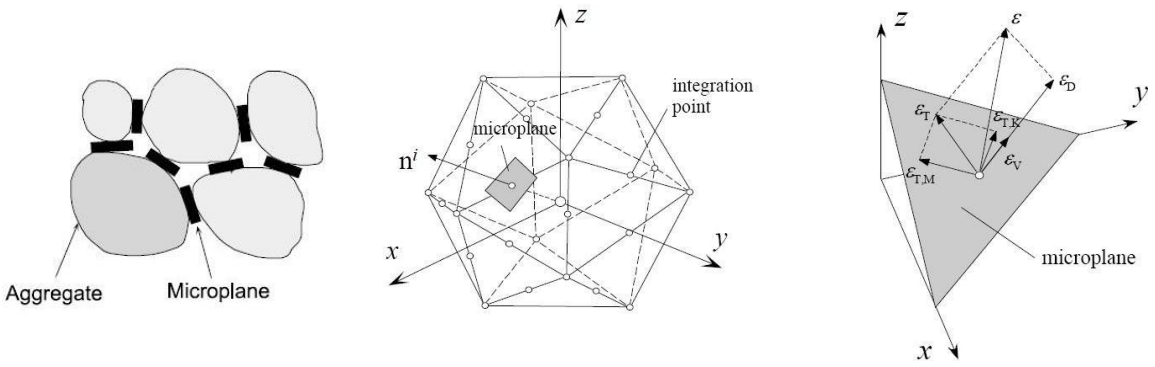

Figure 1.3.1 Microplane model: (a) load transfer over a number of idealized contact planes; (b) FE integration point with 21 microplanes; (c) decomposition of strain vector on the specified microplane. (Ožbolt et al., 2001; Ožbolt et al., 2011)[3]

1.4 Fastening systems

Tension loads can be transfered by fasteners to the base material with mechanical interlock, friction or bond. In case of mechanical interlock, the load is transfered by means of bearing interlock between the fastener and base material. This load-transfer mechanism is realized by headed anchors, anchors channels, screw anchors and undercut anchors.

Friction is employed by expansion anchors. Expansion force is induced during the installation process and that leads to generating a friction force between the anchor and the sides of the drilled hole. This friction force is in equilibrium with the external tensile force.Chemical interlock is the load-transfer mechanism where the tension load is transferred to the base material by means of bond, i.e. some combination of adhesion and micro-keying. This mechanism is employed by bonded anchors.

Fastening systems also differ in the way of their installation. They can be cast-in-place, drilled in and installed directly. Cast-in-place components are secured in the formwork prior to casting. Drilled-in anchors are installed in holes drilled into the hardened base material. Direct installation refers to studs or nails driven into the base material with powder cartridges or pneumatic action. [2]

2. BEHAVIOUR OF USED MATERIALS AT HIGH TEMPERATURES

This chapter will describe the behavior of used materials (concrete and steel), as well as the change of their initial characteristics during elevated temperature. Most building materials change their microstructure and their initial features are rather disturbed.

2.1 Concrete at elevated temperatures

2.1.1 Thermophysical properties of concrete

Thermal expansion

The thermal expansion of unloaded concrete is the thermal strain due to heating. When free to deform, concrete will expand due to temperatureincreasing. Concrete expands slightly as temperature rises. Thermal expansion varies primarily with aggregate type, cementitous material content, water cement ratio, temperature range, concrete age and ambient relative humidity. Of these factors, agregate type has the greatest influence on the expansion. With increased temperature, the main constituents of concrete, cement paste and aggregate, behave differently. Figure 2.1.1.1 shows the thermal contraction and expansion of cement paste and rocks reported by different researchers. The hardened cement paste presents slight expansion at temperatures up to about 150 °C. Afterwards it starts to shrink. However, rocks keep expansion at elevated temperatures.

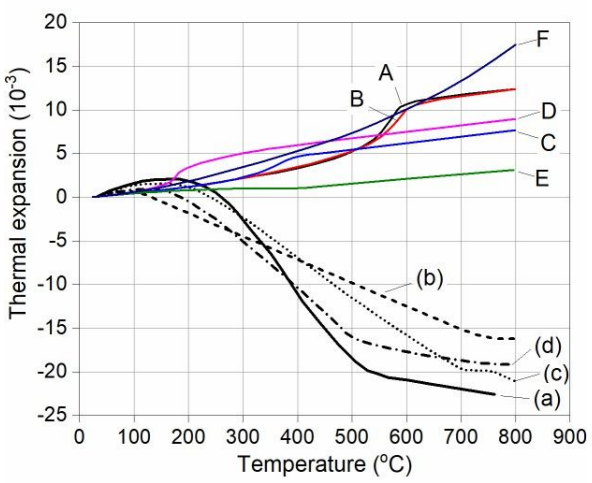

Figure 2.1.1.1Thermal expansion of cement paste: (a) Philleo (1958), (b) Harada et al. (1972), (c) Cruz and Gillen (1980) and (d) Crowley (1956), cited in (Bažant and Kaplan, 1996); and rocks: A andB (sedimentaryrock),C(pyroxene,amphibolite,andesite),D(pyroxene-andesite),E(siliceousrock)andF (limestone).(Haradaetal.,1972). [1]

Thermal conductivity

The thermal conductivity λ is defined as the ratio of the heat flux to temperature gradient. It is important factor when considering the amount of heat transfere through conduction. The moisture content, temperature, type of aggregate, type of cementitious material and density of concrete are influential factors of the thermal conductivity. It is mainly influenced by the type of aggregate since normally aggregates comprise 60-80% of the volume of concrete. More water in concrete leads to higher porosity, resulting in greater volume of air. The thermal conductivity of aggregates and concretes varies in a large range at ambient condition. However, water has comparatively rather low thermal conductivity and air has the lowest. Thus, it makes sense that dense concrete has higher thermal conductivity. With increasing temperature the thermal conductivity of concrete is decreased (Figure 2.1.1.2).At temperatures within 100 °C, the thermal conductivity of concrete is little affected. Thereafter, due to the evaporation of water and the dehydration and decarbonation, a more porous material structure is developed and the thermal conductivity of normal weight concrete is seen decreased gently.[1]

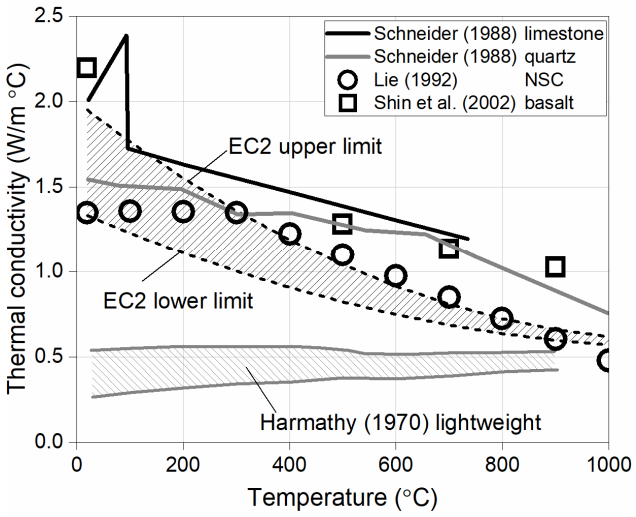

Figure 2.1.1.2 Thermal conductivity of concrete as a function of temperature [1]

2.1.2 Thermomechanical properties of concrete

Compressive strength

The strength of concrete degrades with temperature due to the evaporation of water, loss of bond strength between aggregate and cement paste, dehydration of the hydrated cement products, thermal cracking and so on. The rate of strength degradation is highly influenced by compressive strength of concrete. Up to temperature of 300 °C, compressive strength was reported to be unaffected. After this temperature, compressive strength decreases with increasing temperature. Typically, the compressive strength increases slightly up to 200 °C and then decreases gradually up to 400 °C. Beyond this temperature the compressive strength decreases dramatically. After 800 °C, less than 20% of original strength is left.

The loss of compressive strength at elevated temperatures depends on the concrete mixture of aggregate, the heating-cooling regime, the test conditions, and so on.[1]

The residual strength after cooling of all concrete types retained much lower than that tested in the hot state. This is due to severe thermally induced damage of concrete during the cooling process. The way of cooling has a noticeable influence on the residual strength. It should be noted that maximum difference is reached for temperature ranging from about 400 to 700 °C. After this temperature the difference between hot state strength and cold state strength is small.

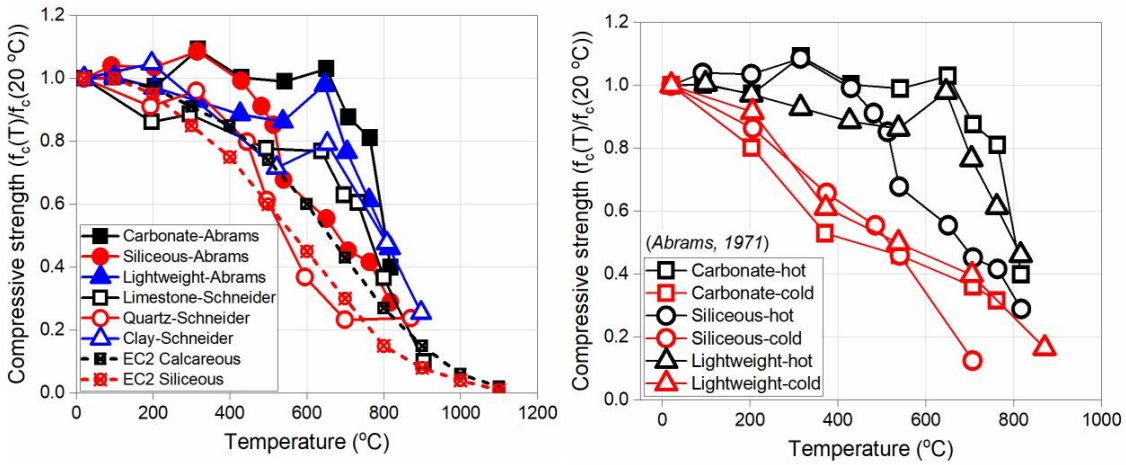

Figure 2.1.2.1 Compressive strength of normal strength concrete as a function of temperature. (a) Values for hot state strength; (b) comparison between the hot state and cold state strength [1]

Young's modulus

The modulus of elasticity (E) of various concrete materials at room temperature varies over a wide range, and is dependant mainly on the water-cement ratio in the mixture, the age of concrete, the method of conditioning, and the amount and nature of the agregates.

Figure 2.1.2.2 shows the reduction of Young's modulus of normal strength concrete with increasing temperature. The Young's modulus decreases monotonically.The modulus of elasticity of normal weight concretes decreases at a higher pace with the rise of temperature than that of lightweight concretes.The comparison of the Young's modulus obtained from hot state test and cold state test is illustrated in Figure 2.1.2.2 b. It is obvious the residual Young's modulus after cooling is much lower than that tested in the hot state.

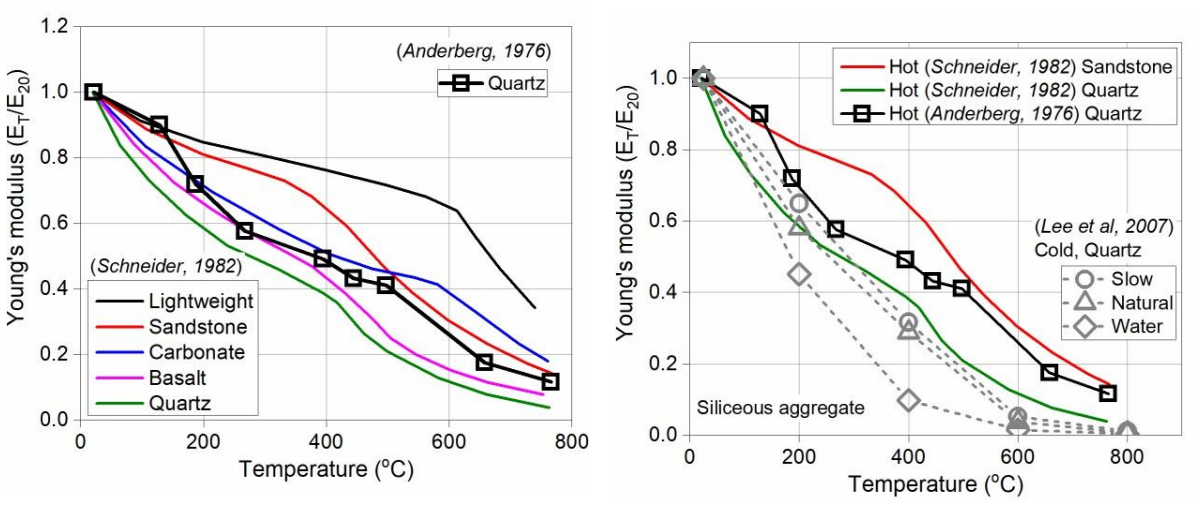

a) *b)*

Figure 2.1.2.2 Young's modulus of normal strength concrete as a function of temperature. (a) Values for hot state; (b) comparison between values of hot and cold state. [1]

Tensile strength

The tensile strength of concrete is much lower than that of compressive strength (less than 10% of the compressive strength), and hence tensile strength of concrete is often neglected in strength calculations at room and elevated temperatures and instead the capacity of steel under tension is utilized. However, from fire resistance point of view, it is an important property, because cracking in concrete is generally due to tensile stresses and the structural damage of the member in tension is often generated by progression in microcracking. The fasteners in concrete mainly make use of the tensile strength of concrete. It is therefore important to understand the evolution of concrete tensile strength with increasing temperature.

In the Eurocode 2 Part 1-2 it is assumed that up to 100 °C the tensile strength is unaffected and it decreases linearly to zero at 600 °C (European Committee for Standardization, 2004a) (slika 3.8.a)) Figure 2.1.2.3 presents a comparison of the evolution of tensile strength of normal strength concrete tested in the hot and cold state with increasing temperature. It is seen that the hot state strength is slightly larger than the cold state strength. However, they follow very similar reduction tendency. [1]

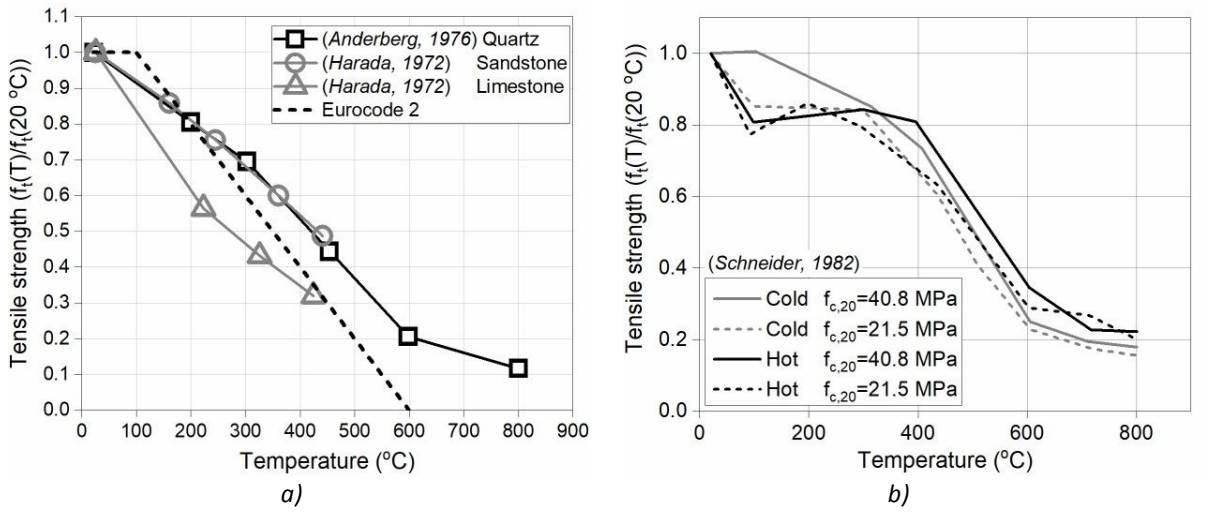

Figure 2.1.2.3 Tensile strength of normal strength concrete as a function of temperature. (a) Values for hot state; (b) comparison between values for hot and cold state. [1]

Fracture energy

The fracture energy is defined as the amount of energy necessary to create one unit area of crack. It is usually measured by means of stable three-point bending tests on notched concrete beams or wedge-splitting test, in which the applied load and the crack mouth opening displacement (CMOD) need to be monitored continually. This makes an appropriate measurement in the hot state difficult and no data of fracture energy in the hot state could be found. At ambient temperature, many discussions have been conducted on the fracture energy of concrete. The influence of high temperature on the fracture energy of concrete can only be evaluated after cooling, i.e. in the cold state. (Yu et al., 2013) performed the wedge-splitting test to investigate the temperature on the fracture energy of concrete. The temperature considered ranging from ambient to 600 °C. Figure 2.1.2.4a shows the effective load on crack development as a function of the CMOD after exposing the concrete specimens to different temperatures. It is seen that the peak load is reduced with increasing temperature. (Baker, 1996) and (Zhang and Bicanic, 2002) studied the influence of high temperature on the fracture energy of concrete by conducting the three-point bending tests. Both of them observed that the fracture energy increased with increasing temperature and then decreased, with maximum values at 300 °C [1]

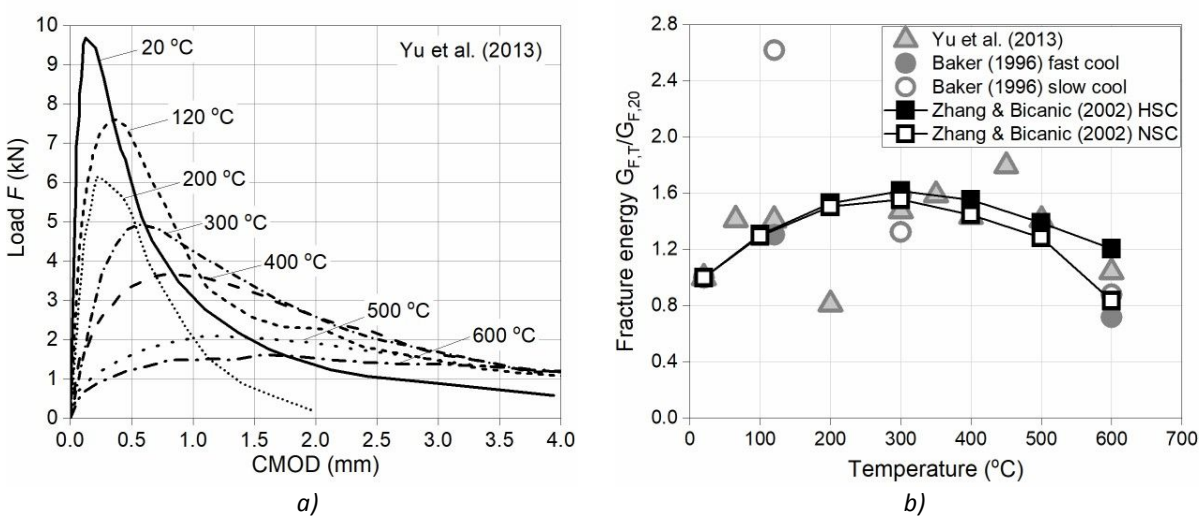

Figure 2.1.2.4 (a) Effective load as a function of CMOD after exposing concrete to various temperatures; (b) relative fracture energy as a function of temperature from different researchers.[1]

2.1.3 Thermal strain

The thermal strains of concrete at elevated temperatures can be divided into free thermal strain and load induced thermal strain.The free thermal strain (FTS, ε_{th}) stands for the strain that is developed when unloaded concrete is under heating. Since the thermal stain measurements are performed with unsealed specimens, the free thermal strain includes shrinkage. In Figure 2.1.3.1it is seen that the aggregates type and the proportion of aggregates in concrete affect the free thermal strain the most. The free thermal strain is also a nonlinear function of temperature.[1]

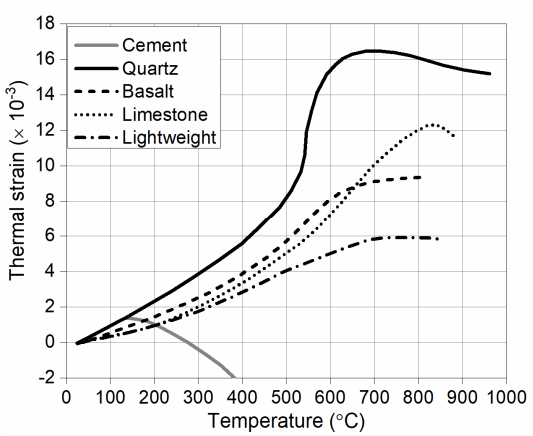

Figure 2.1.3.1Free thermal strain of cement and concrete with different aggregates (Schneider, 1988)

The load induced thermal strain (LITS) is the difference of strain between the thermal strain of not loaded specimen and the strain of a concrete specimen loaded with constant load applied prior to heating *(fédération internationale du béton (fib), 2007)*. Figure 2.1.3.2 shows the straintemperature curves of concrete specimens heated while loaded with 0%, 10%, 20% and 30% load. Based on the meso-scale simulations of concrete, it has been shown that the main reason for LITS is the interaction between free thermal strain and load induced damage of cement paste (Bošnjak, 2014).[1]

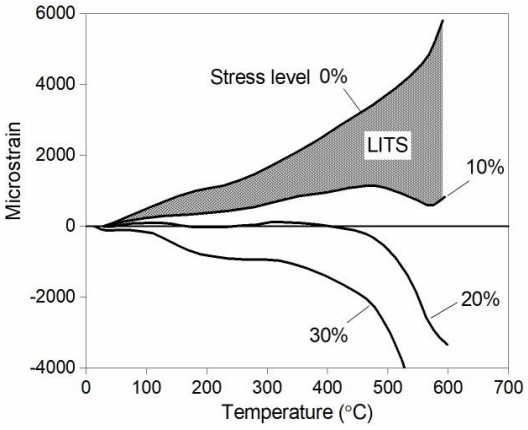

Figure 2.1.3.1 LITS for concrete heated with 1 °C /min under 0%, 10%, 20% and 30% load, in the figure the LITS for 10% load is explicitly marked (Khoury, 2006)

2.2 Steel at elevated temperatures

In the hot state, the strength of steel degrades pronouncedly with increasing temperature (Kordina and Meyer-Ottens, 1981). According to (Harmathy, 1993), at 650 °C only 20% and 10% of original strength is left for hot-rolled and cold-drawn steel, respectively. In the model the reduction of Young's modulus and yield strength is accounted for, as plotted in Figure 2.2.1.

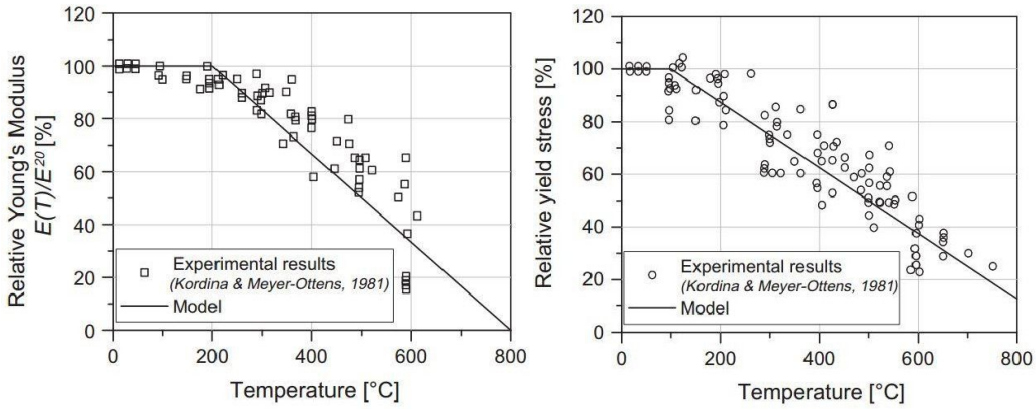

Figure 2.2.1 Comparison of experimental data and the model for (a) relative Young's modulus and (b) relative yield strength of steel as a function of temperature in the hot state (Ožbolt et al., 2013).

Studies on the residual strength of steel after cooling show that, unlike concrete, steel can recover its yield strength depending on the type of steel (*Takeuchi et al.*, 1993; *Felicetti and Meda*, 2005).(*Felicetti and Meda*, 2005) showed that the residual strength of deformed bars are up to 550 °C almost completely recovered. Furthermore, the residual Young's modulus of steel is equal to the value of virgin steel. Figure 3.18 shows the recovery of the yield stress of steel as implemented in the model.[1]

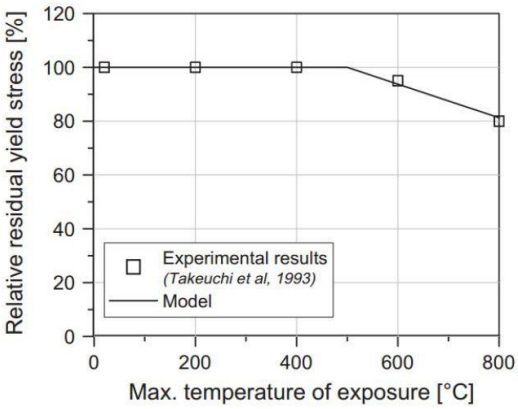

Figure 2.2.2 Comparison of experimental data and the model for relative residual yield strength of steel as a function of temperature in the cold state (Ožbolt et al., 2013).

3. MODELING AND GEOMETRIC CHARACTERISTICS

3.1 Parametric study

The influence of three different edge distances (c1 = 75 mm, 100 mm and 150 mm), two anchor diameters (d = 16 mm and 25 mm) and two embedment depths (hef = 75 mm and 95 mm) on the response of the model were investigated. Both the hot and cold states after 15 min, 30 min and 60 min of fire exposure for concrete grade C20/25 were considered.Dimensions of the concrete element are 4.63 x 5.0 x 3.0 (m) and they are kept constant for each model.All models are shown in Table 3.1.

Table 3.1. List of models

Anchor	Edge distance c/mm	Embedment depth h_{ef}/mm	Stud diameter d/mm	Fire duration (min)
c75h75d16	75	75	16	15; 60
c75h75d25	75	75	25	15; 60
c100h75d25	100	75	25	15; 60
c150h75d25	150	75	25	15; 60
c75h95d25	75	95	25	15; 30; 60
c100h95d25	100	95	25	15; 30; 60
c150h95d25	150	95	25	15; 30; 60

3.2 Overview of used materials and their characteristics

This chapter describes materials used in model design and calculation along with properties and other characteristics of a particular material. The two main materials used in modeling are concrete and steel, but because of the way of modeling and the requirements of the computer program, 6 characteristics is used to describe them. The materials were chosen to match the materials used in the experimental tests (K.Tian, 2018) for a comparison of results.

Remark: Due to the easier understanding of material properties, each of them is briefly explained in the following table

Concrete	- represents concrete cube
Steel	- represents anchor and rod parts
Contact (plate)	- represents contact elements in contact with concrete and anchor head
Contact (anchor-head)	- represents contact elements in contact with anchor body and anchor head
Contact (anchor-concrete)	- represents contact elements in contact with anchor body and concrete
Bar	- represents the bond between concrete and steel

Table 3.2. List of used materials

Material	Young's modulus E (GPa)	Poisson´s ratio υ_c	Uniaxial compressive strength f_{cm}(MPa)	Tensile strength f_{ctm} (MPa)	Fracture energy G_F (J/m^2)	Heat conductivity λ_c (W/mK)	Heat capacity c_p (J/kgK)	Weight density ρ(kg/m^3)
Concrete C20/25	27	0,18	30	2,9	60	1,49	900	2267
Steel	200	0,33	/	550- 750		18	500	7900
Contact (plate)	10^{-30}	0,33	/		10	10	1	7900
Contact (anchor-head)	200	0,33	/			18	500	7900
Contact (anchor-concrete)	10^{-30}	0,33	/			10	1	7900

Material	Young's modulus E (GPa)	Poisson´s ratio υ_c	Bar area (mm^2)	Tensile strength f_{ctm} (MPa)	Fracture energy G_F (J/m^2)	Heat conductivity λ_c (W/mK)	Heat capacity c_p (J/kgK)	Weight density ρ(kg/m^3)
Bar	1	/	1 mm^2			1	1	1

3.2.1 Anchors

The furnace temperature is heated up to 900 ^{o}C after fire duration of 60 min and over 700 ^{o}C after heating up to 15 min according to ISO 834 fire. Normally used structural steel begins to soften around 420 ^{o}C and loses 90% of its initial strength above 800 ^{o}C (European Committee for Standardization, 2005a). Therefore, the special high-temperature resistant steel 1.4828 according to EN 10095 (European Committee for Standardization, 1999) was used to prevent steel failure in the fire tests carried out at high temperature.Since the aim of the analysis was to investigate the failure of concrete, the behaviour of steel was assumed to be linear elastic. The anchor and the rod are made of steel with Young´s modulus 200 000.00 N/mm^2, and Poisson's ratio 0.33.

3.2.2 Concrete specimens

It is known that high strength concrete is more prone to explosive spalling at high temperatures than normal strength concrete. Because of this, in experimental tests*(Kaipei Tian; Experimental study on concrete edge failure of single headed stud anchors after fire exposure)*is used concrete C20/25 in order to assure concrete failure and to prevent explosive spalling.As is evident from the displayed properties of the material, used concrete has tensile strength 2.90 N/mm^2, compressive strength 30.00 N/mm^2. Young´s modulus is 27000.00 N/mm^2 and Poisson's ratio is 0.18.

3.3 Geometry and finite element discretization

This chapter will describe the procedure of creating the model with geometric characteristics and the way of discretization of the finite element mesh. The finite element discretizationis performed according to the geometry and boundary conditions from the experimental tests by employing 4-node constant strain solid finite elements. The connection between steel and concrete is performed by using contact elements that can transfer only compressive contact forces. Since the aim of the analysis was to investigate the failure of concrete, the behaviour of steel was assumed to be linear elastic.

When designing the model in the Femap computer program, because of simlicity and symmetry, only one half of the concrete element is modeled. For research purposes sveral models have been made in dependance of anchor geometry and concrete edge distance. The mesh is shown only for one model with a single anchor (c75h75d25).

Table 3.3 List of models

Anchor	Edge distance c/mm	Embedment depth h_{ef}/mm	Stud diameter d/mm
c75h75d16	75	75	16
c75h75d25	75	75	25
c100h75d25	100	75	25
c150h75d25	150	75	25
c75h95d25	75	95	25
c100h95d25	100	95	25
c150h95d25	150	95	25

3.3.1 Geometry and finite element discretization of single anchor model

The geometry of the numerical model is based on the actuall dimensions of the model from the experiment. It's corresponding to a concrete element with a headed anchor near the edge. The dimensions of concrete element are 4.63 x 5.0 x 3.0 (m).

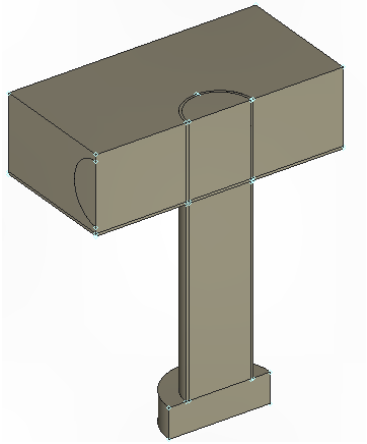

Figure 3.3.1.1 Anchor geometry

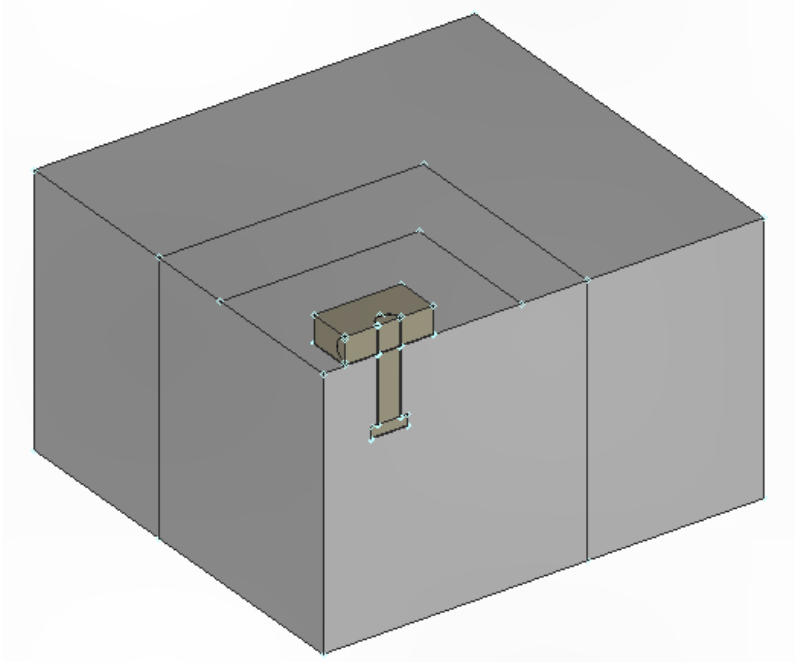

Figure 3.3.1.2 Geometry of single anchor model c75h75d25

Once the entire geometry of the model is completed and the desired shape is achieved, the finite element mesh can be made by describing these two prequisites properly and by having the corresponding property assigned to them.

The first step in designing the finite element mesh is to define and create all materials. Then, using the geometry of the model, the number of finite elements can be defined (mesh size).

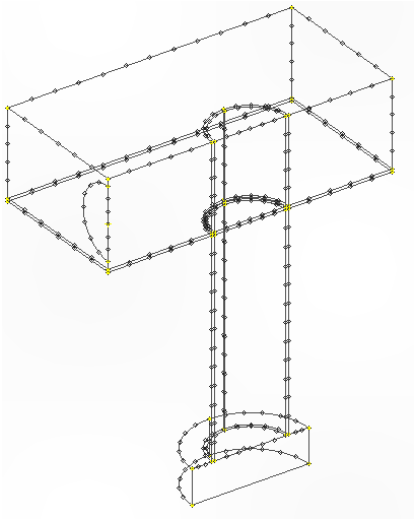

Figure 3.3.1.3 Mesh size of an anchor

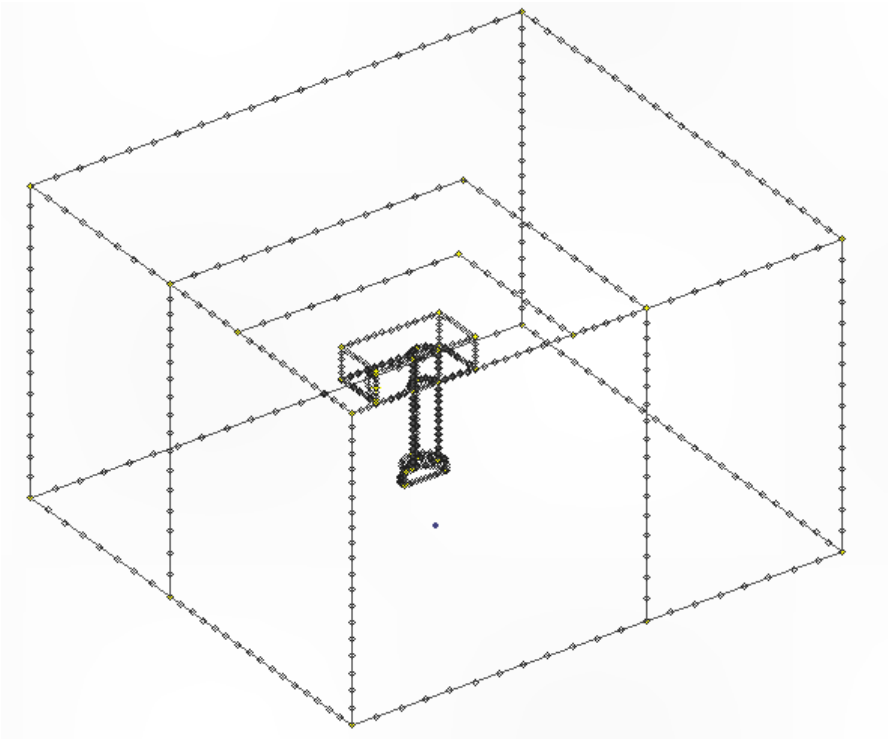

Figure 3.3.1.4 Mesh size of a single anchor model c75h75d25

After assigning the number of elements to each line of geometry, a mesh of three-dimensional (3D) finite elements can be made. One layer of 1 mm tickness elements, defined later as contact elements, is modeled around the anchor.. Their purpose is to model the surface zone between concrete and anchor, i.e. for simulating the connection between these two materials.The contact elements can only transfere shear and compressive stresses. As for spatial discretization of steel (except head of an anchor), three-dimensional elements with 8 knots and 8 integration points (hexagonal 3D finite elements) were used.

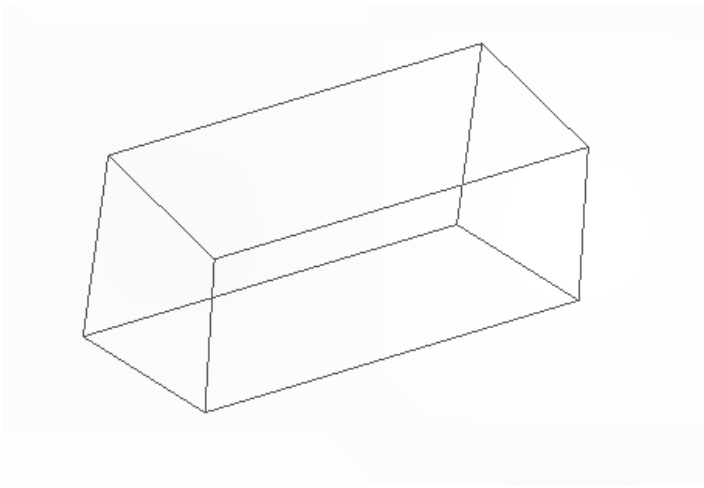

Figure 3.3.1.5 Hexagonal three-dimensional (3D) finite element

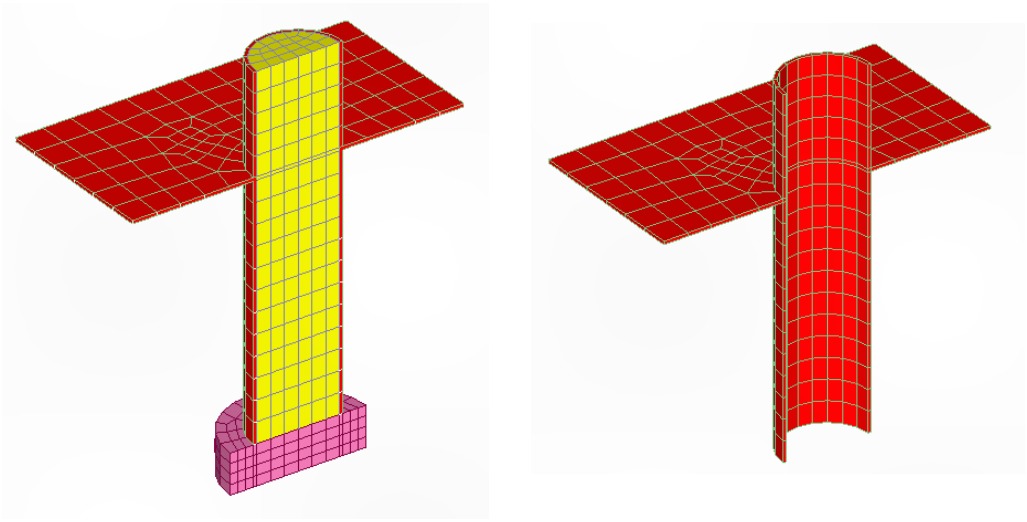

a) *b)*

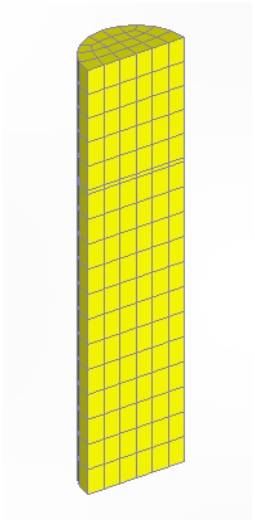

c)

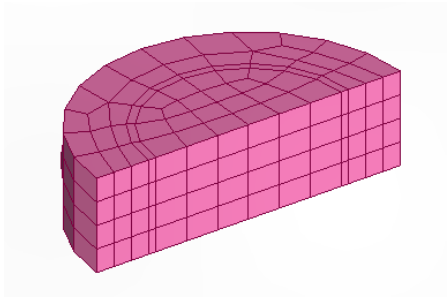

d)

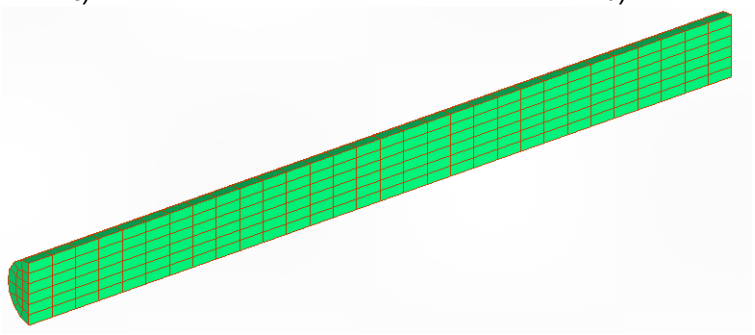

e)

Figure 3.3.1.6a) Entities with hexagonal 3D finite elements; b) Contact elements; c) Anchor elements; d) Anchor.head elements; e) rod elements

The spatial discretization of the concrete and the anchor head elements was made with tetrahedral three-dimensional (3D) finite elements with 4 nodes and 4 integration points.

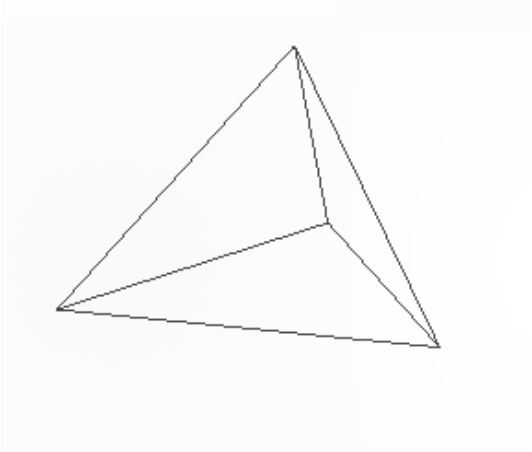

Figure 3.3.1.7 Tetrahedral three-dimensional (3D) finite element

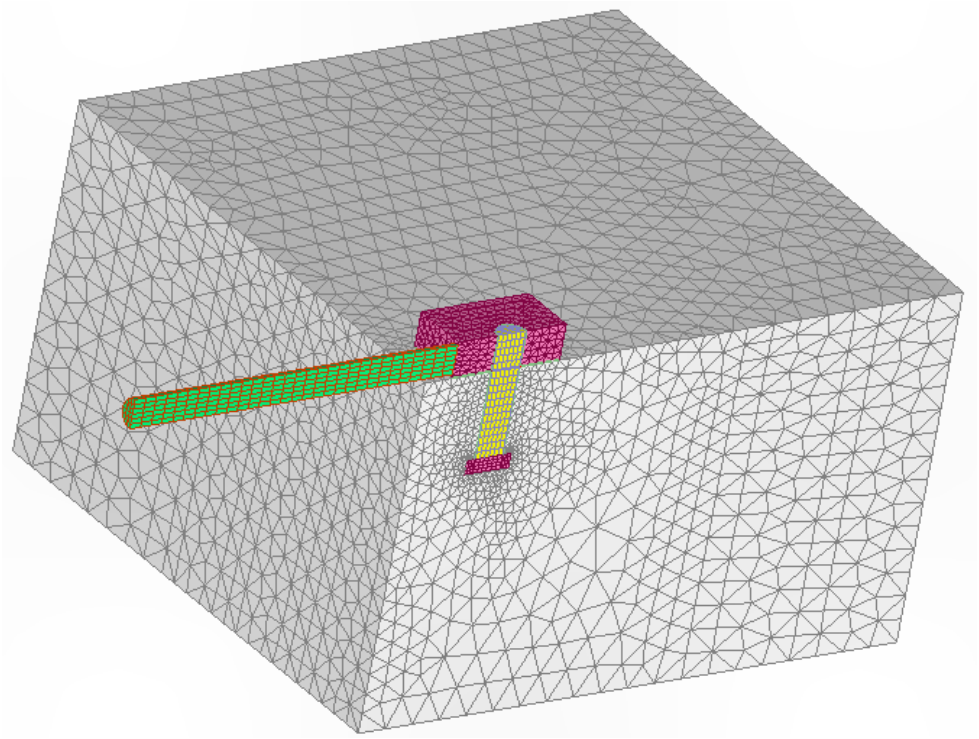

Figure 3.3.1.8Finished model finite element mesh

For model testing and research purposes after meshing the geometry, it is necessary to assign the load to the model and to set the boundary conditions, which will be described in chapters 3.4 and 3.5

3.4 Initial and boundary conditions

This chapter describes setting initial and boundary conditions of the model. Boundary conditions are equally set on each model, therefore the constraints are shown only for one model. The Femap® program visualizes the constraints in a way that in the chosen point draws a small triangle with the number 1, 2 or 3 depending on the direction of the restricted motion (1-restricted displacement in X direction; 2-restricted displacement in Y direction; 3-restricted displacement in Z direction). In order to model the symmetry on the body, the constraints with restricted displacements in X direction (perpendicular to the plane) were set on the plane which cuts the anchor in half. To make the system staticly determined, on a top right and down back edge of the concrete element are set constraints with restricted displacements in Z direction, and on the back left edge are set constraints with restricted displacements in Y direction (reactions will be measured here).

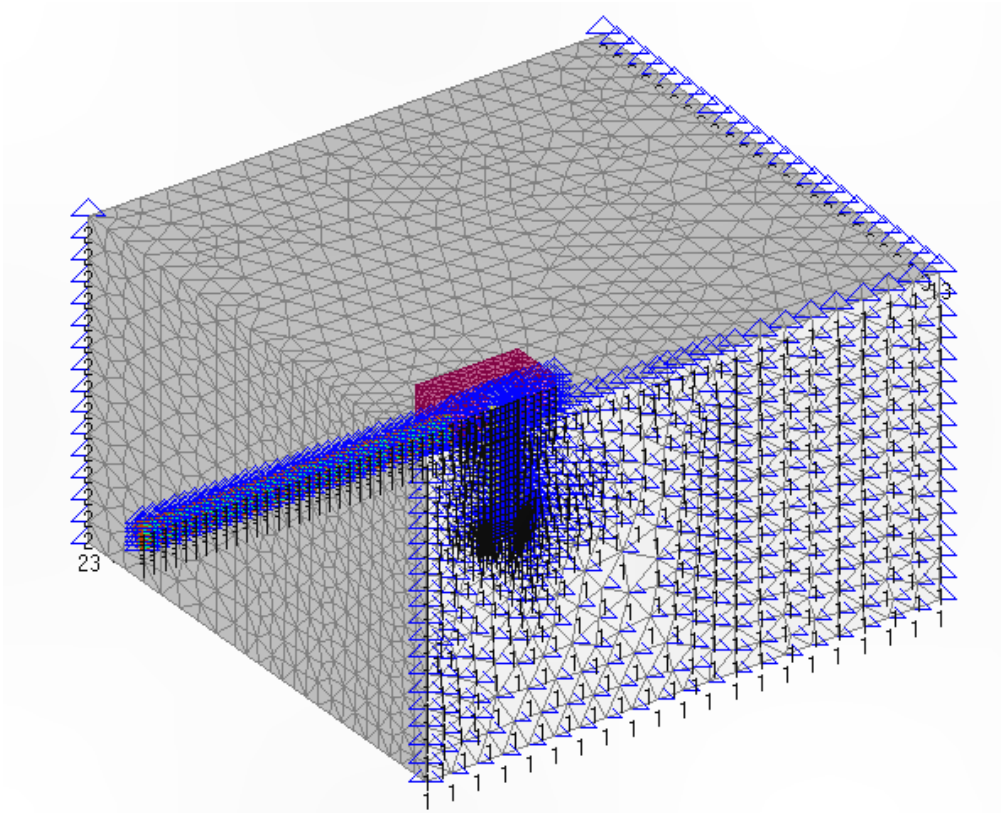

Figure 3.4.1 View of constraints in nodes of the model from the front (1-restrained displacement in X direction; 2-restrained displacement in Y direction; 3-restrained displacement in Z direction)

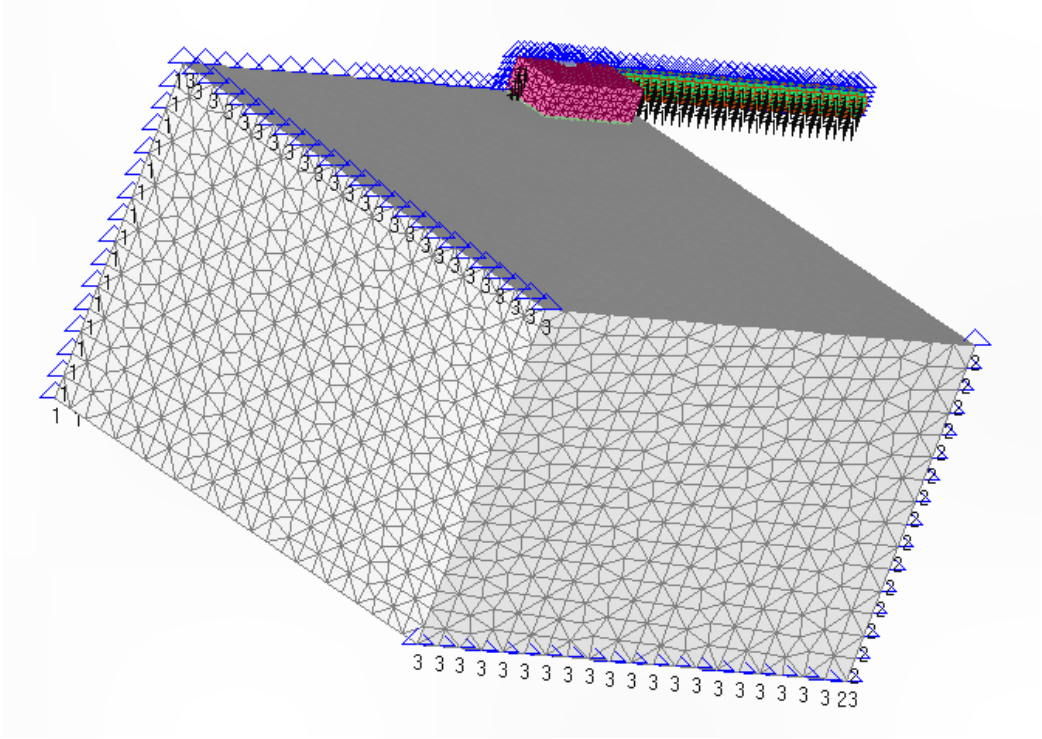

Figure 3.4.2 3D View of constraints in nodes of the model from the back (1-restrained displacement in X direction; 2-restrained displacement in Y direction; 3-restrained displacement in Z direction)

3.5 Thermal and mechanical loads

In order to preform a thorough analysis and to account forinfluences of different loading conditions, the loading process was divided into 3 phases:

- 1. phase - preloading: shear load perpendicular to the edge
- 2. phase - high temperature exposure
- 3. phase - displacement until failure

All models presented are loaded in 2 ways:

First one contains all 3 phases. Models are first loaded in shear perpendicular to the edge (phase1). Then follows exposure to high temperature in phase 2. The considered fire duration times in this phase were 15 and 60 min. In the 3rd phase, the method of pulling the anchor perpendicular to the edge is made in such way that the small increments are set in the given numbers of steps.

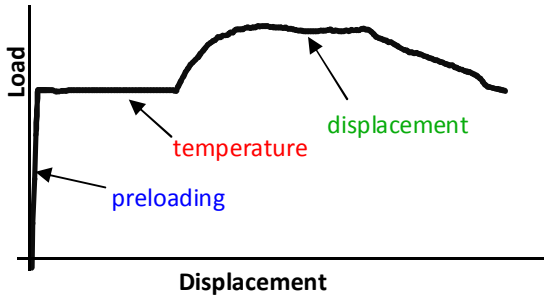

Figure 3.5.1. Typical load-displacement curve for all 3 phases of loading (preloading + high temperature exposure + displacement until failure)

The second way of loading the models is without preloading. It consists of phase 2 and phase 3. The models are first exposed to high temperature, and then the anchor is pulled perpendicular to the edge until concrete failure.

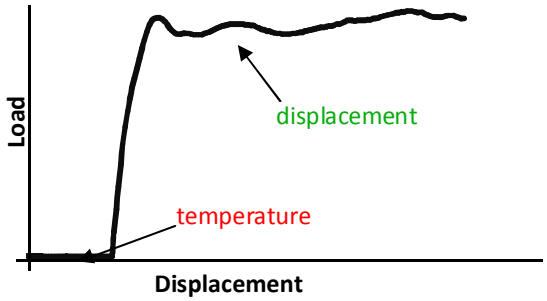

Figure 3.5.2. Typical load-displacement curve for 2 phases of loading (high temperature exposure + displacement until failure)

Since all models are loaded in the same way, the loading procedure will be shown in detail for only one model. The results of the simulations and their comparison will be shown in chapter 4 (Results).

3.5.1 Phase 1 - preloading: shear load perpendicular to the edge

If the anchor loaded in shear is placed near the edge of a concrete element, and if that shear load is perpendicular to the edge, that may lead to concrete failure before the load-carrying capacity is reached. It is established by experimental researches that the fracture crack develops at angle of 35° on the surface of element, and increases with depth to 1.3 - 1.5 times the edge distance. The load-bearing behaviour of such fasteners depends on the behaviour of concrete in tension, which is described by CC-Method. [2]

Based on the experimental and numerical research on headed studs and post-installed bonded anshors, an equation for predicting the average concrete failure load of a single anchor subjected to a shear load applied perpendicular to the edge is made:

$$V_{u,c}^{0} = 2.4 \cdot d_{nom}^{\alpha} \cdot l_f^{\beta} \cdot f_{c,c\,200}^{0.5} \cdot c_1^{1.5} \quad [\mathrm{N}] \tag{3.1}$$

where:

$$\alpha = 0.1 \cdot \left(\frac{l_f}{c_1}\right)^{0.5}$$

$$\beta = 0.1 \cdot \left(\frac{d_{nom}}{c_1}\right)^{0.2}$$

d_{nom} = outside diameter of a post-installed anchor, or shank diameter *d* of a headed stud [mm]
≤ 25 mm

c_1 = edge distance, measured from the longitudinal axis of the anchor

l_f = effective load transfer length [mm]
= h_{ef} for anchors with constant flexural stiffness over the lenth of the anchor
= length of the embedded distance sleeve for post-installed anchors with a non-uniform flexural stiffness (i.e. sleeve-type anchors)

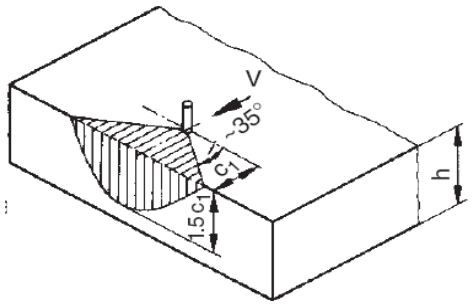

Figure 3.5.1.1 Anchor loaded in shear towards an edge (after Fuchs, Eligehausen(1995)). Idealised shape of typical concrete failure body[2]

According to equation (3.1), concrete failure load of a near-edge shear loaded anchor is influenced by the edge distance, anchor diameter, concrete strength and l_f.Comparing with experimental values, the failure loads predicted by the equation are almost identical for standard applications ($d \leq 20$ mm and $c_1 \leq 200$ mm). [2]

Calculated values of concrete failure load for a near edge shear loaded anchor are shown in a table for every model.

Table 3.4. Concrete failure load

Anchor	Edge distance c/mm	Embedment depth h_{ef}/mm	Stud diameter d/mm	Concrete failure load $Vuc,0$/kN
c75h75d16	75	75	16	12,63
c75h75d25	75	75	25	13,6
c100h75d25	100	75	25	19,67
c150h75d25	150	75	25	33,48
c75h95d25	75	95	25	14,43
c100h95d25	100	95	25	20,74
c150h95d25	150	95	25	35,02

This load, once applied, is present throughout the complete process of model testing and is simulated in a way that is gradually applied in 5 steps. After its maximum preload value has been reached, model is exposed to high temperature (phase 2).

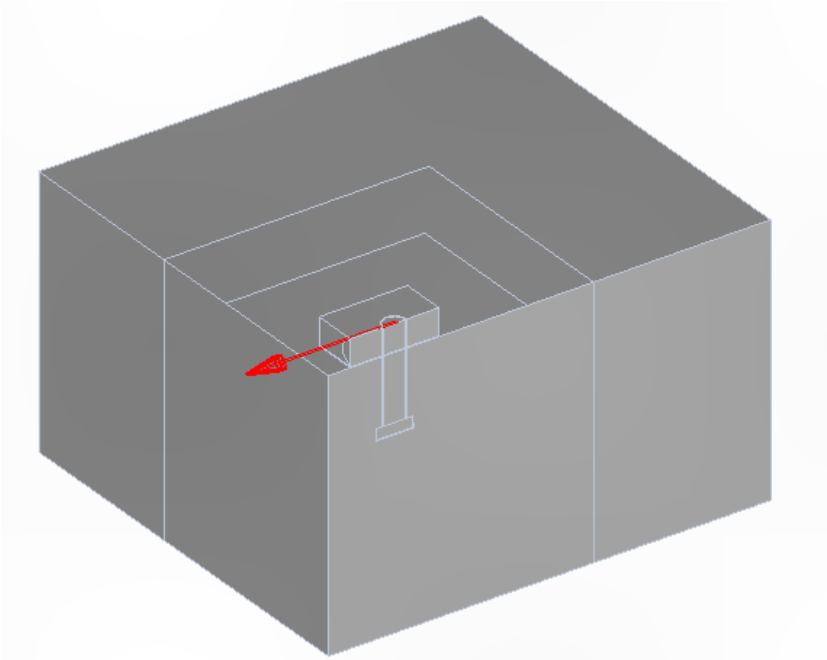

Figure 3.5.1.2 Near edge anchor loaded in shearperpendicular to the edge (-Y direction)

3.5.2 Phase 2 - high temperature exposure

In the second phase the model is exposed to high temperature on two surfaces, in the same way as it was conducted in the experiment.

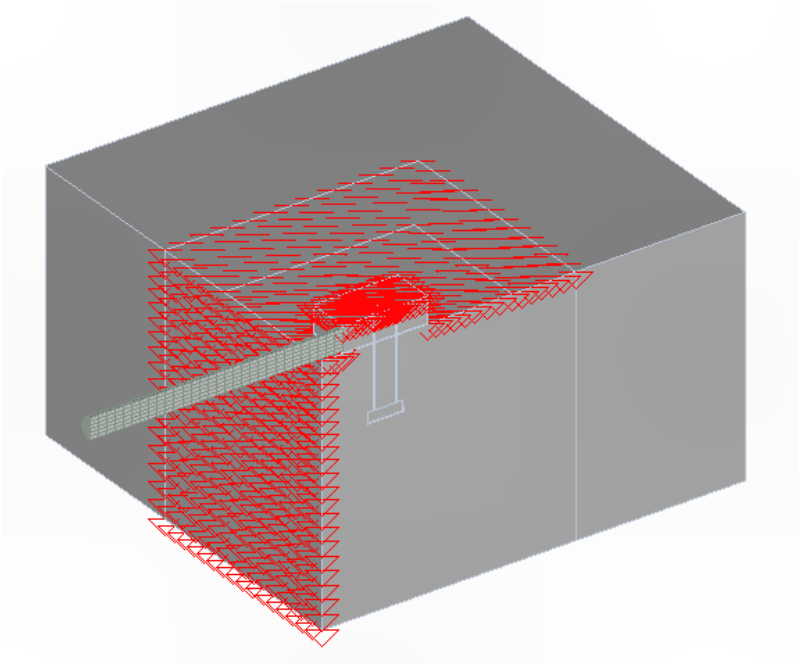

Figure 3.5.2.1 Temperature load

This phase is furher divided in two loading cases. In the first case, the element starts to warm up based on the standard temperature-time curve ISO-834 (15 and 60 minutes) and immediately after that, phase 3 is followed. In the second case, following the heating phase, the model is cooled down to the room temperature of 25°C. The temperature gradient of the cooling curve depends on how pre-heated the element is. The element is heated to standard temperature-time curve ISO-834, according to which the temperature increases rapidly in the first half an hour to about 800 °C, and then in the next 90 minutes reaches 1050 °C.

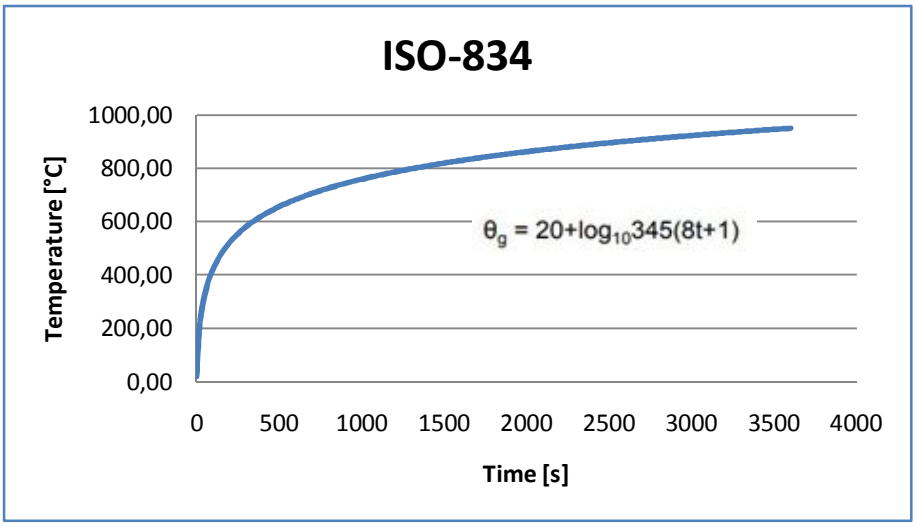

Figure 3.5.2.2 Standard temperature-time curve ISO-834

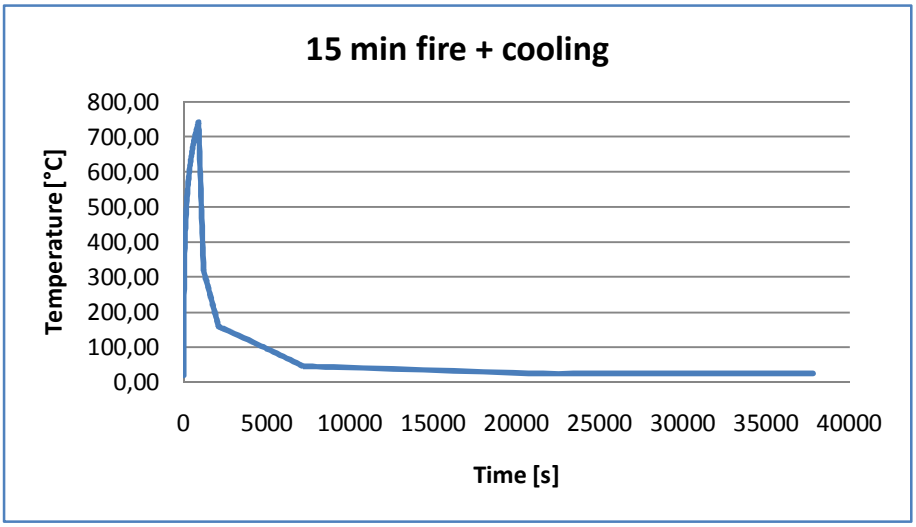

Figure 3.5.2.3 Temperature-time curve for 15 min fire and cooling

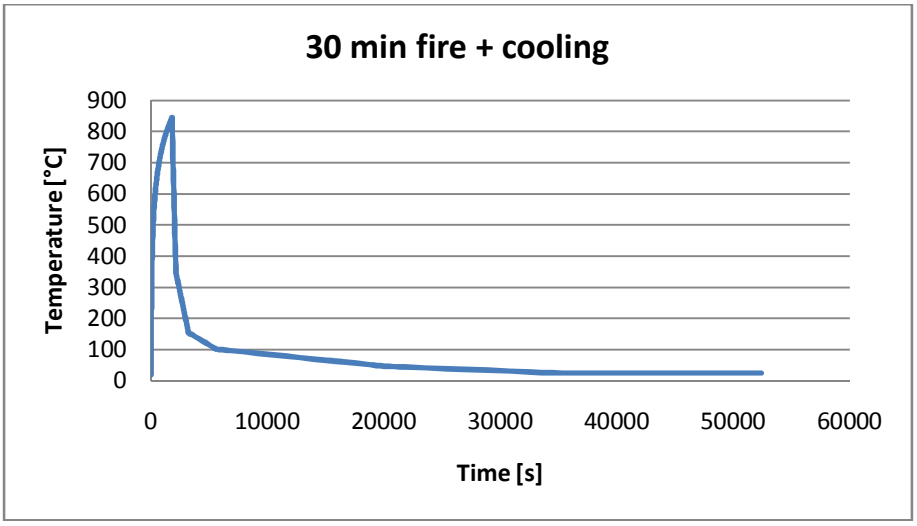

Figure 3.5.2.4 Temperature-time curve for 30 min fire and cooling

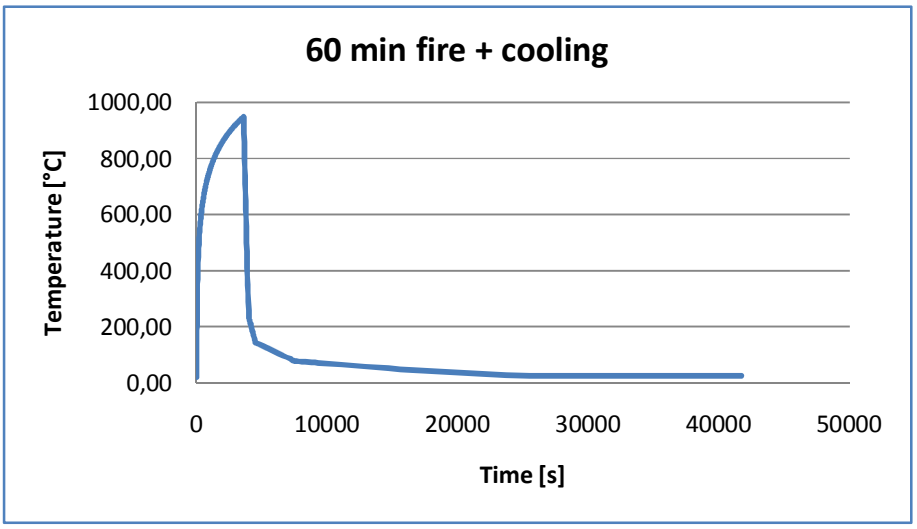

Figure 3.5.2.5 Temperature-time curve for 60 min fire and cooling

The load in this phase consists of the temperature load set in the nodes of the finite elements and the heat flux load which is placed on the outer surfaces of the finite elements.

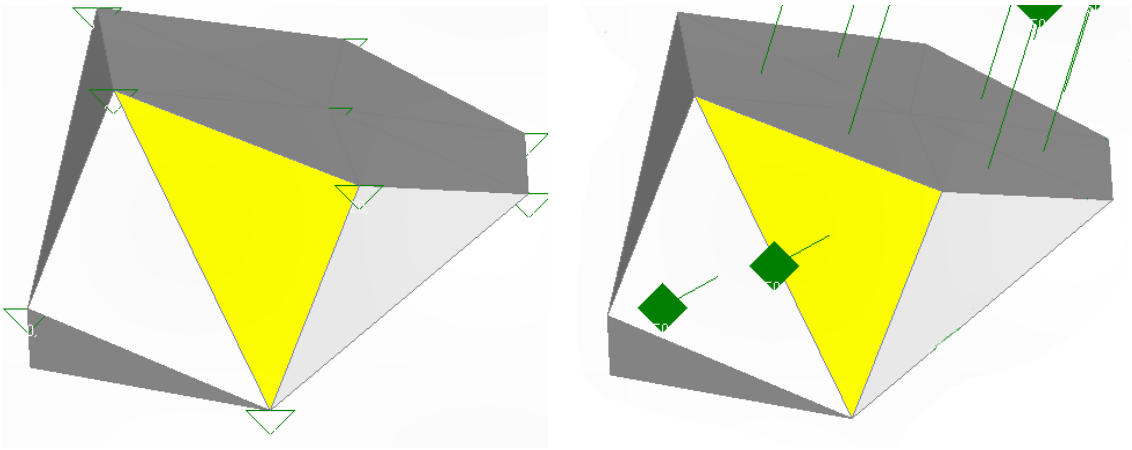

Figure 3.5.2.6 a) Temperature load defined in nodes of finite elements; b) Heat flux load defined on the outer surfaces of the finite elements

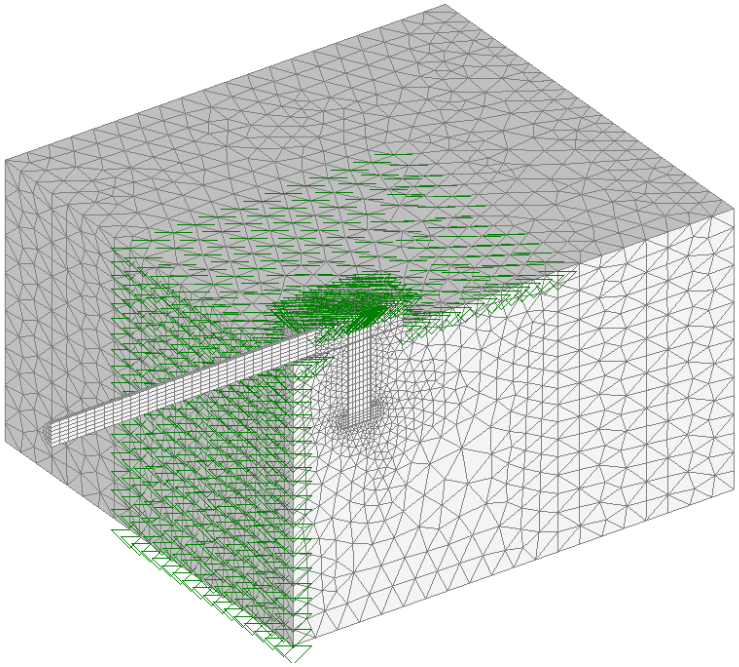

Figure 3.5.2.7 Surfaces exposed to high temperatures

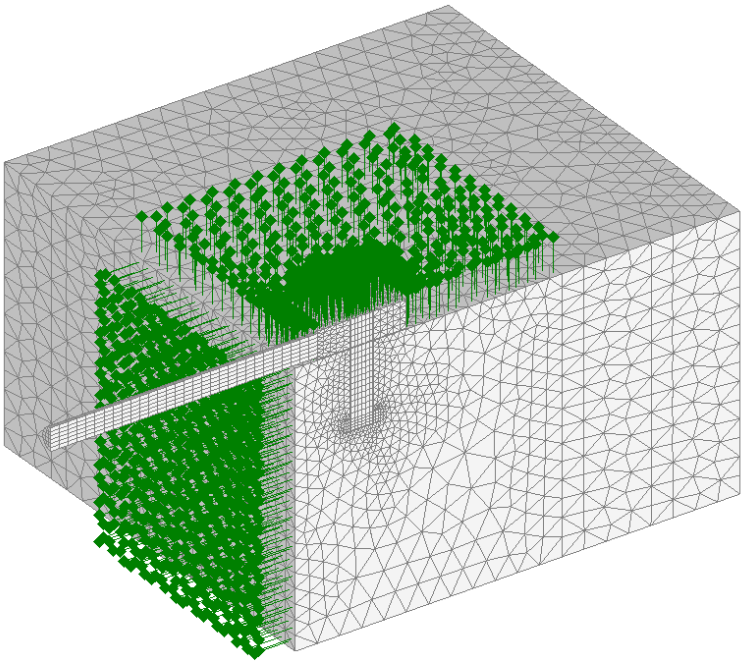

Figure 3.5.2.8 Surfaces exposed to heat flux

3.5.3 Phase 3 - displacement until failure

The load in phase 3 is controlled by displacements set on front side of the rod. In this way, the maximum reactions before failure in constrained nodes could be monitored.

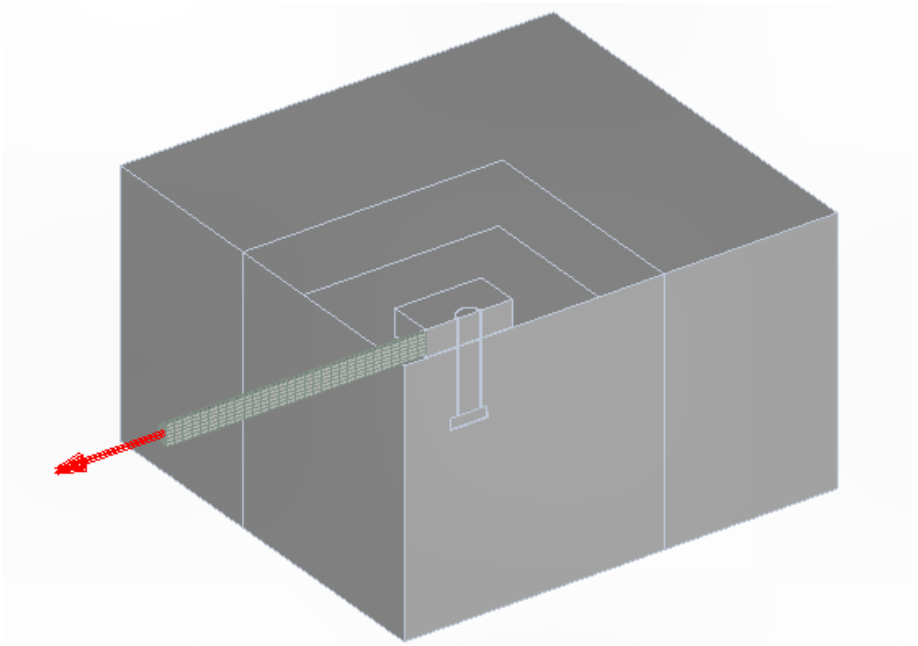

Figure 3.5.3.1 Displacement set on front side of rod (-Y direction)

This type of analysis is an incremental process and the load has to be divided into a number of steps. Each step uses the default number of iterations. Number of steps has to be chosen carefully so the failure load can be established with sufficient accuracy. In each step, a displacement of 0.02 mm is made.

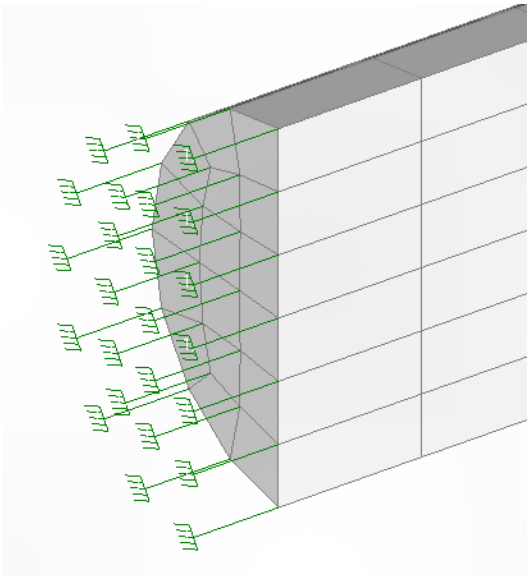

Figure 3.5.3.2 Displacement set in nodes on front side of the rod (-Y direction)

4. RESULTS

A list of numerically tested models with adjacent geometry and fire duration times is shown below. Three different edge distances (c1 = 75 mm, 100 mm and 150 mm), two anchor diameters (d = 16 mm and 25 mm) and two embedment depths (hef = 75 mm and 95 mm) were investigated. Both the hot and cold states after 15 min, 30 min and 60 min of fire exposure were considered for models with embedment depth h_{ef} = 95 mm. Models with embedmenth depth h_{ef} = 75 mm were tested for 15 and 60 fire duration, both the hot and cold state.

Table 4.1 List of models with associated fire durasions

c_1 (mm)	h_{ef}(mm)	d (mm)	Fire duration $fi(t)$ (min)
75	75	16	15; 60
75	75	25	
100	75	25	
150	75	25	
75	95	25	15; 30; 60
100	95	25	
150	95	25	

4.1 Numerical results

The results obtained numerically by using earlier described programs MASA and FEMAP will be presented in this chapter. The load-displacement curves are shown for each model in dependance of the preloading existence (with or without preloading), fire duration (15 min, 30 min and 60 min) and fire state (hot and cold state). Later the results were compared considering diferent edge distance, embedment depth and diameter of an anchor, as well as the preloading existence. The results obtained numerically are also compared with those obtained experimentally by (K.Tian, 2018) to verify the numerical prediction.

4.1.1 Load-Displacementcurves for pull-out (phase 3) without temperature exposure and preloading

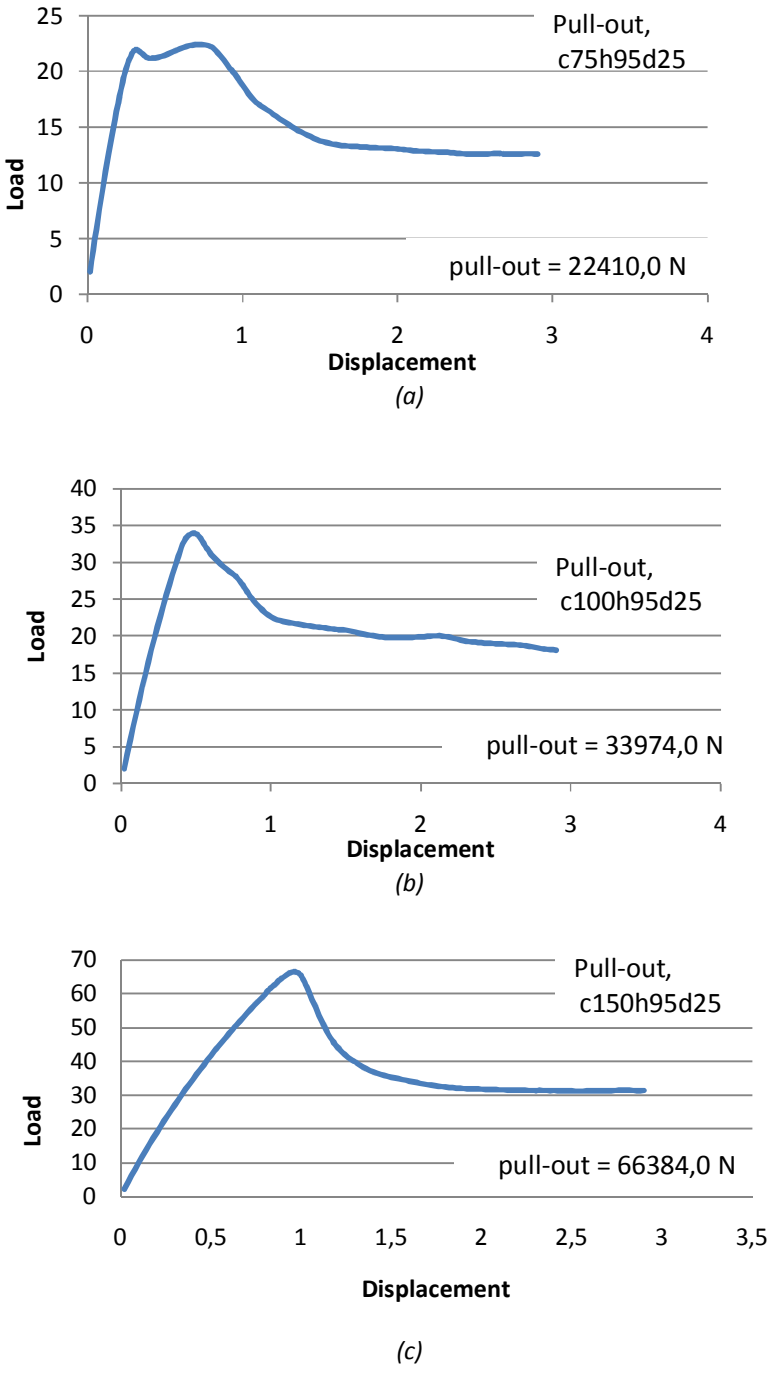

Figure 4.1.1.1 Load-displacement curves for pull-out (a) model c75h95d25; (b) model c100h95d25; (c) model c150h95d25;

4.1.2 Load-Displacement curves in the cold and hot state

Representative load-displacement curves for anchorage configurations in Table 3.1 are presented in this section to show comparisons between the load-bearing behaviour in the cold and hot states. The anchor resistance in the case of concrete edge failure after fire exposures of 15, 30 and 60 min was found to be higher for the cold state than the hotstate. It is known that the concrete edge failure resistance is mainly dependent on the edge distance, but after fire exposure, the embedment depth and diameter of an anchor may play a significant role. Therefore, the following numerical load-displacement curves considering these factors are presented. Figure 4.1.2.1 shows the numerical load-displacement curves of single headed stud anchors in both the hot and cold states after 15 min, 30 min and 60 min of fire exposure for concrete grade C20/25.For all configurations peak load in the cold state is higher comparing to that in the hot state.

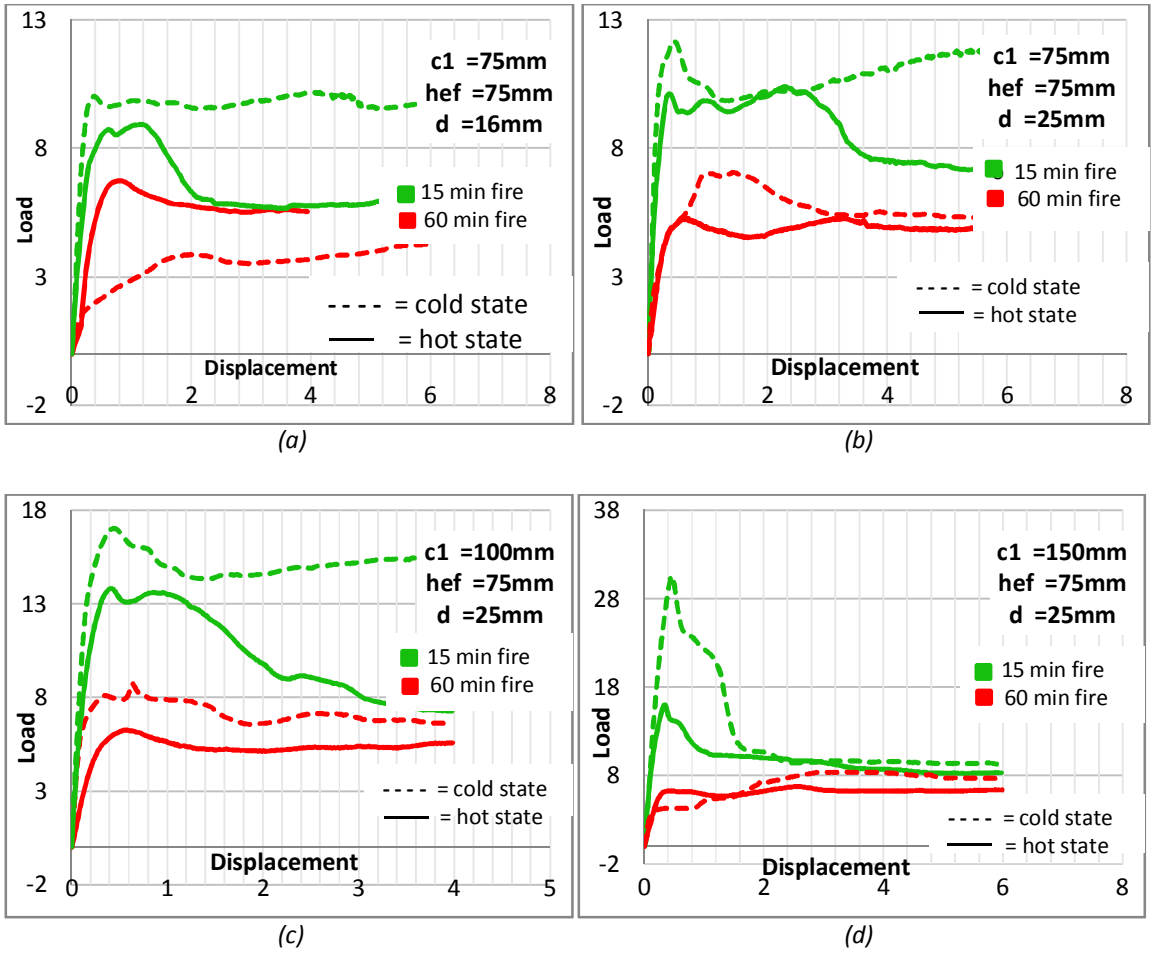

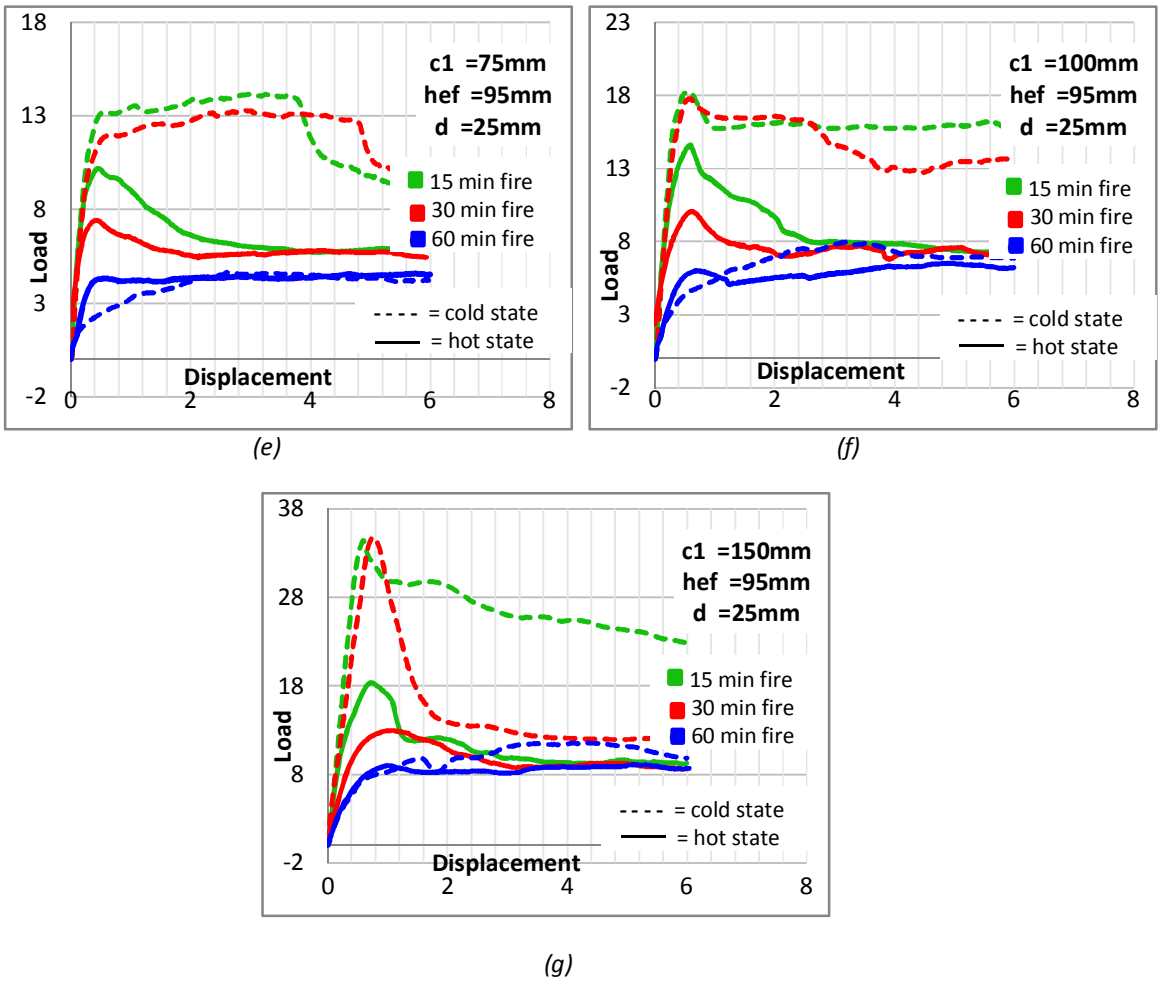

Figure 4.1.2.1 Load-displacement curves for cold and hot state for each model (a) model c75h75d16; (b) model c75h75d25; (c) model c100h75d25; (d) model c150h75d25; (e) model c75h95d25; (f) model c100h95d25; (g) model c150h95d25

It is worth noting that the anchors exposed to 15 min and 30 min of fire duration show similar resistance in the cold state. Anchors with greater embedment depth also show similar resistances for cold and hot states after 60 min of fire exposure, unlike 30 min of fire exposure where differences between hot and cold state are significant.

4.1.3 Load displacement curves for phases with and without preloading

Preloading, as it turnes out, plays an important role in bearing capacity of anchors exposed to fire. Firstly, the anchor was preloaded to design load and kept constant, then the heating was conducted with fire exposure of 15 min, 30 min and 60 min followed by the cooling phase. Afterwards the anchors were loaded until failure. According to EN 1990 (European Committee for Standardization, 2002) and the Technical Specification (European Committee for Standardization, 2009a), the calculated design load for the anchors: c75h75d16 (c1 = 75 mm, hef = 75 mm and d = 16 mm), c75h75d25, c100h75d25, c150h75d25, c75h95d25, c100h95d25 and c150h95d25 were 12.63 kN, 13.6 kN, 19.67 kN, 33.48 kN, 14.43 kN, 20.74 kN, and 35.02 kN, respectively.

Table 4.1.3.1 Calculated design load

Anchor	Edge distance c/mm	Embedment depth h_{ef}/mm	Stud diameter d/mm	Concrete failure load $Vuc,0$/kN
c75h75d16	75	75	16	12,63
c75h75d25	75	75	25	13,6
c100h75d25	100	75	25	19,67
c150h75d25	150	75	25	33,48
c75h95d25	75	95	25	14,43
c100h95d25	100	95	25	20,74
c150h95d25	150	95	25	35,02

For the purposes of drawing the following diagrams, only parts of the real load-displacement curves have been displayed.

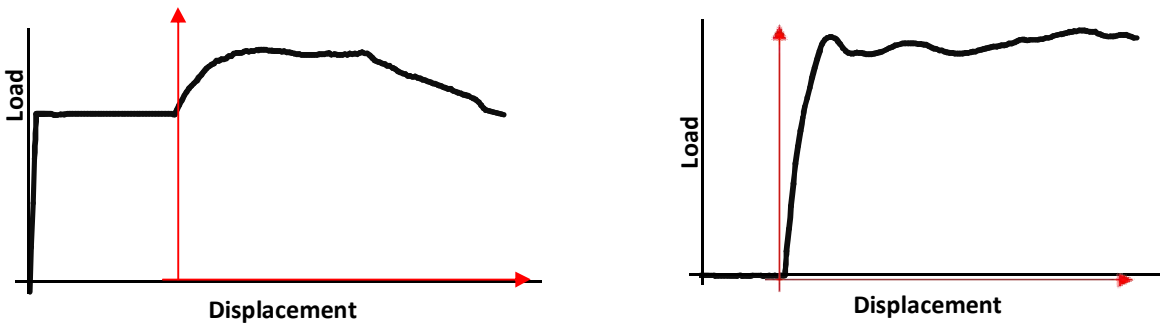

(a) *(b)*

Figure 4.1.3.2 Simplification of phase 3 display (displacement until failure)

The following diagrams show a behaviour of anchors, with and without preloading exposed to different fire durations. It is obvious that preloading causes significant reduction of resistance, especially in cold state where reduction is up to about 80 %. It is also evident that, in hot state, with increasing fire duration, the reduction of resistance is increasing as well, which is different for cold state where the reduction decreses with increasing fire duration (except for model c75h75d25).

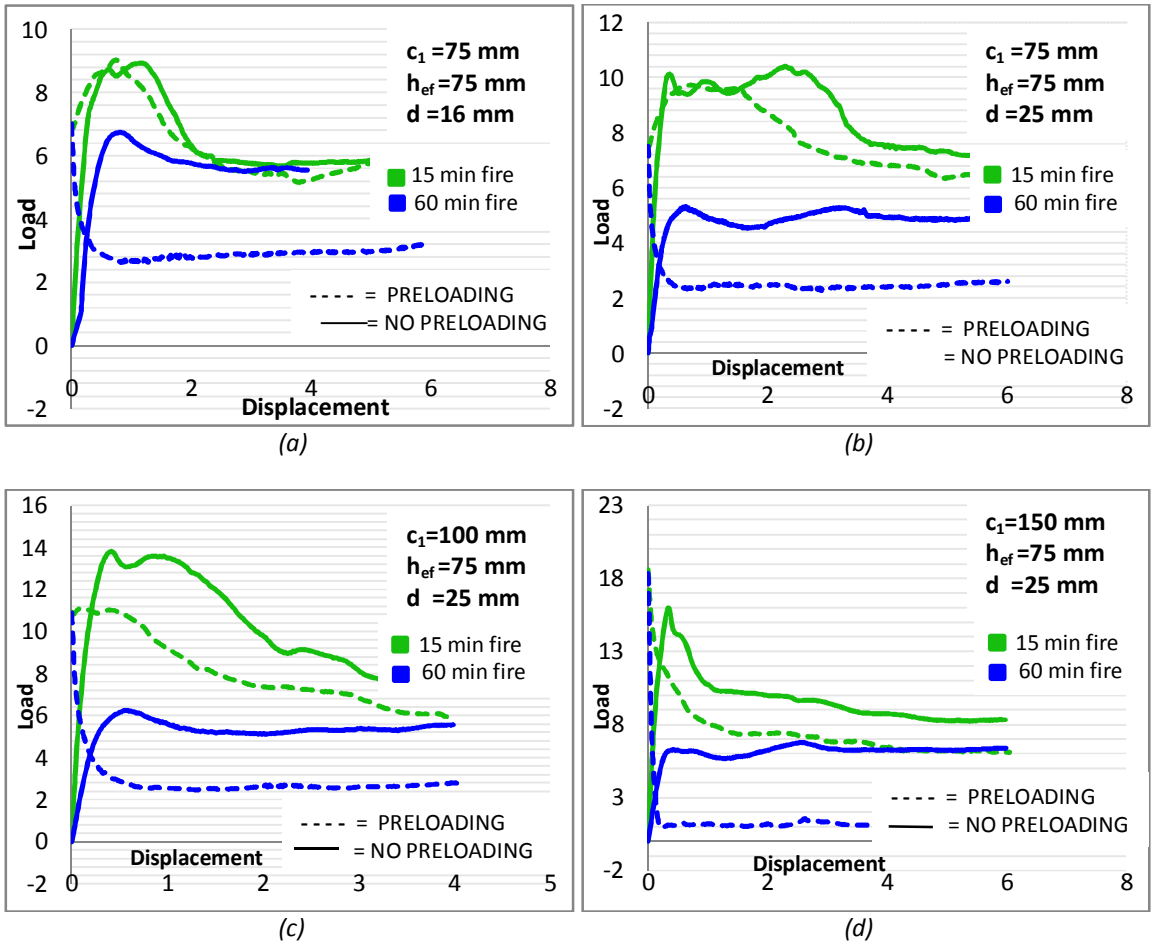

Figure 4.1.3.3 Load-displacement curves for hot state of preloaded and not preloaded models with 15 and 60 min fire duration (a) c75h75d16; (b) c75h75d25; (c) c100h75d25; (d) c150h75d25

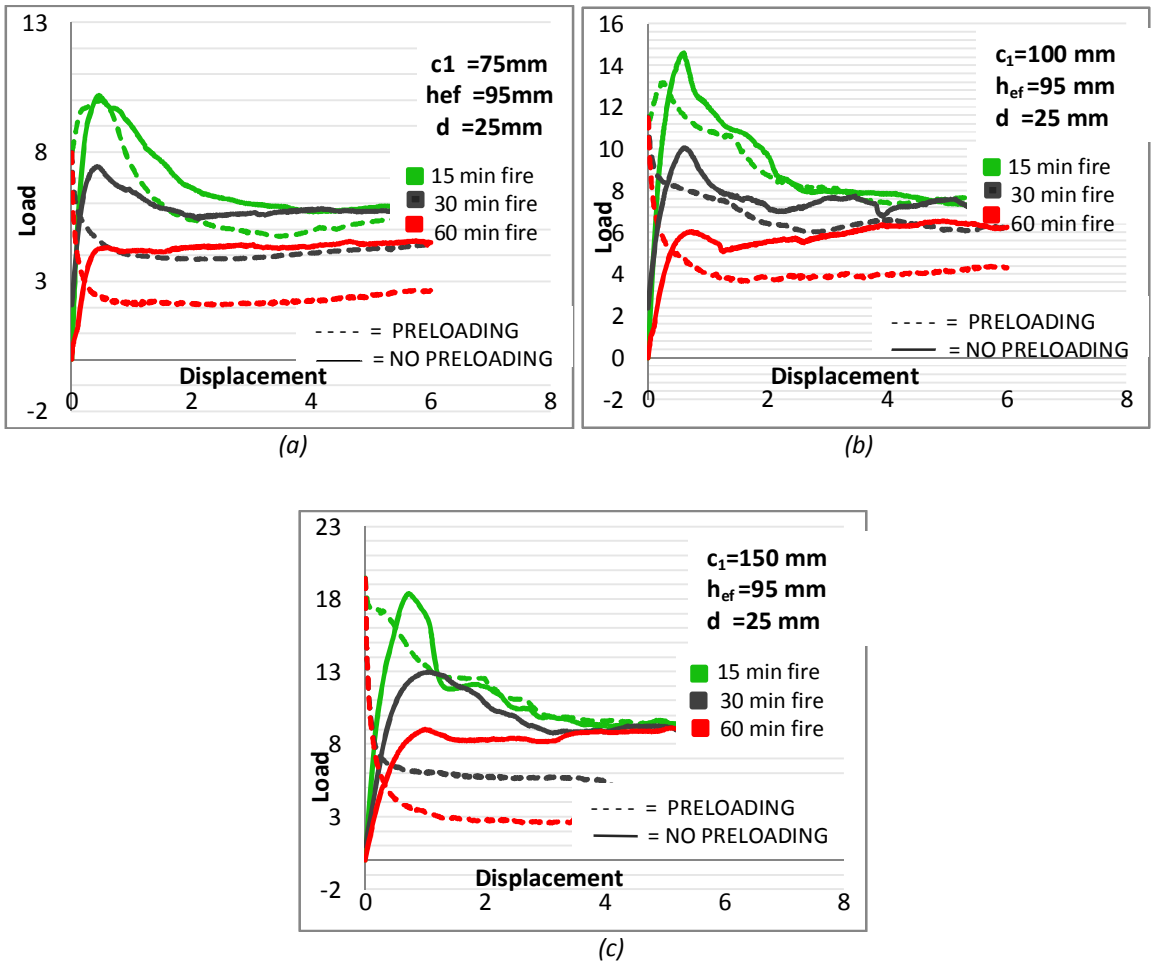

Figure 4.1.3.4 Load-displacement curves for hot state of preloaded and not preloaded models with 15, 30 and 60 min fire duration (a) c75h95d25; (b) c100h95d25; (c) c150h95d25;

In the hot state, anchors exposed to 15 min fire duration, do not show any major changes in bearing capacity due to preloading. The situation is different for anchors exposed to 60 min fire duration and the bearing capacity decreases significantly due to preloading. In most cases, bearing force shows a sudden decrease immediately after fire exposure which tells us that the concrete edge failure happened already in the second phase of loading (temperature exposure). In those cases, bearing capacity of anchors after fire exposure is extremely low.

The greatest decrease of bearing capacity due to preloading is indicated by anchors with a larger edge distance (c_1=150mm) where the resistance after 60 min of fire exposure decreases by up to 80% from the resistance of not preloaded anchor. Anchors set closer to the edge (c_1=75mm) manifest the decrease of about 55% after 60 min fire exposure due to preloading.

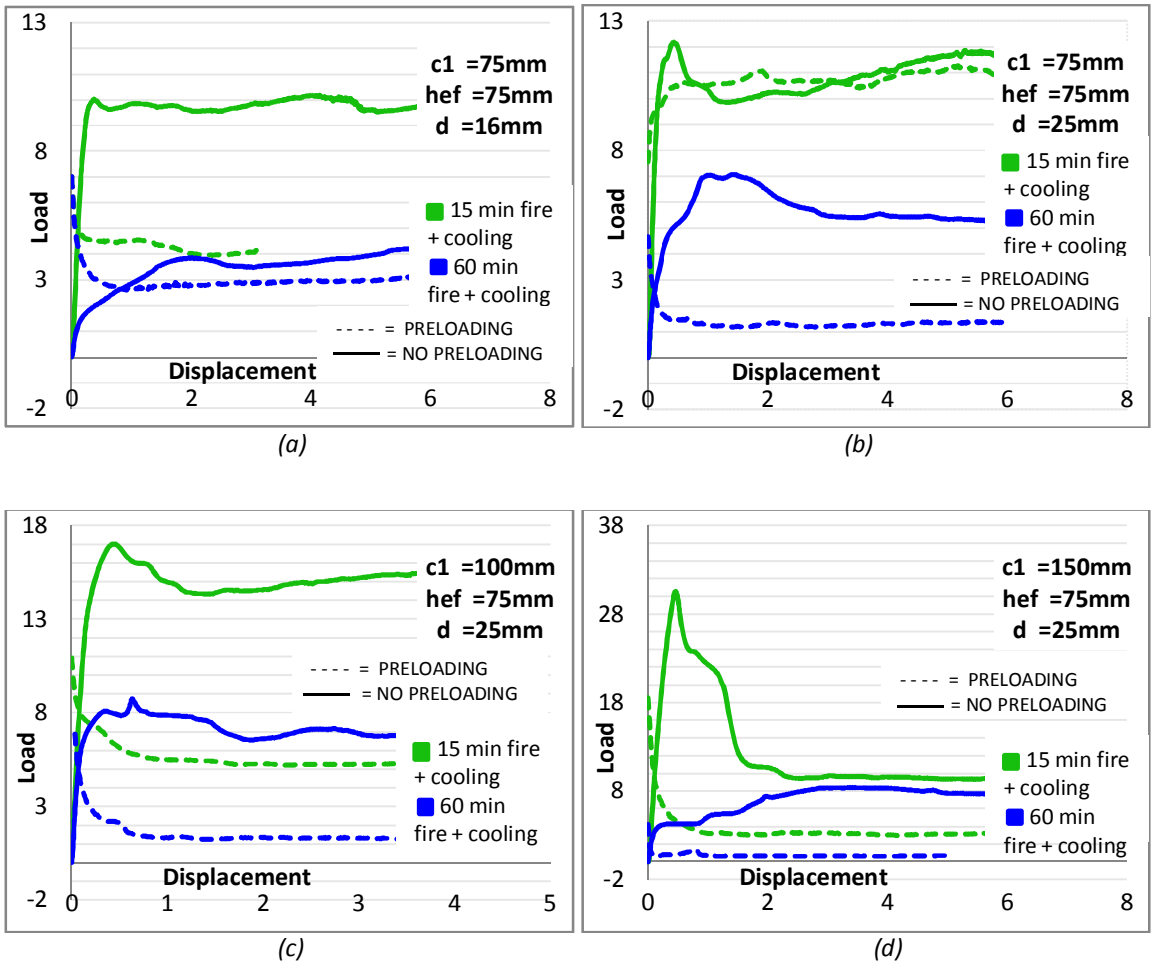

Figure 4.1.3.5 Load-displacement curves for cold state of preloaded and not preloaded models with 15 and 60 min fire duration (a) c75h75d16; (b) c75h75d25; (c) c100h75d25; (d) c150h75d25

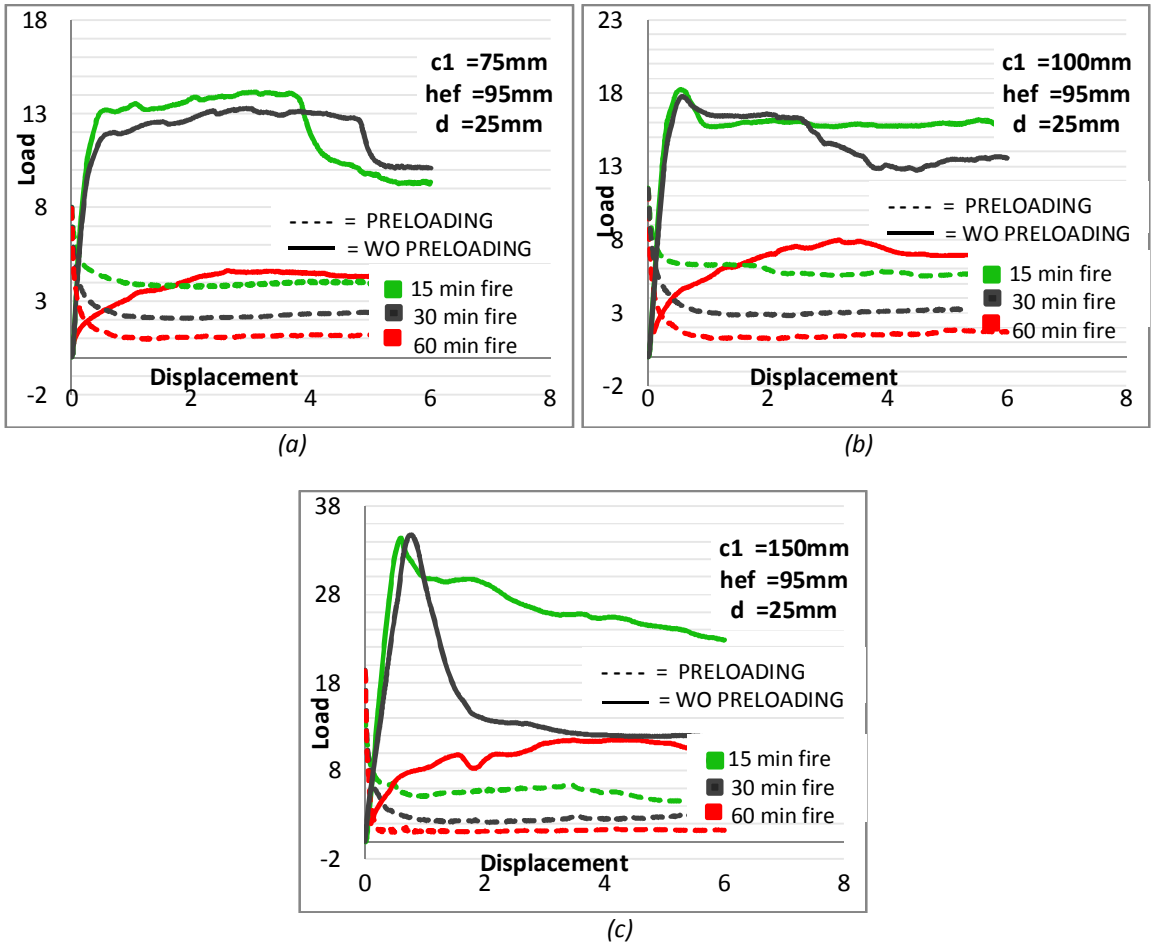

Figure 4.1.3.6 Load-displacement curves for cold state of preloaded and not preloaded models with 15, 30 and 60 min fire duration (a) c75h95d25; (b) c100h95d25; (c) c150h95d25;

Unlike the hot state, the cold state shows a greater reduction of bearing capacity due to preloading, especially after 15 min and 30 min of fire exposure. Comparing the resistances of preloaded anchors with diferent edge distances, it can be seen that the resistances in cold state become more similar with increasing edge distances. Bearing capacity decreases with increasing fire duration and the diffrences between preloaded and not preloaded anchors are getting smaller.

In many cases, because of preloading, concrete edge failure happens in phase 2 where the model is still heating up. On the beginning of phase 3 (pulling the anchor until failure), a sudden reduction of resistance is evident.

4.1.4 Peak load

In this chapter the load bearing capacities of headed stud anchors loaded in shear perpendicular to the free edge after fire exposure of 15 min, 30 min and 60 min of standard fire curve ISO 834 are numerically investigated. The effect of concrete edge distances c_1 of 75 mm, 100 mm and 150 mm, together with the influence of different nominal diameter d_{nom} of 16 mm and 25 mm, and embedment depth h_{ef} of 75 mm and 95 mm on the load-bearing behaviour of the anchors at various durations of fire were taken into account.

Concrete failure occured mainly in phase 3 where the rod was pulled out until failure of concrete. However, in some cases the concrete failure occured in second phase where the model is still heating up, especially in cases where the anchor was preloaded.All peak loads obtained are shown in figures 4.1.4.2 and 4.1.4.3. Corresponding displacements at peak loads are also indicated.

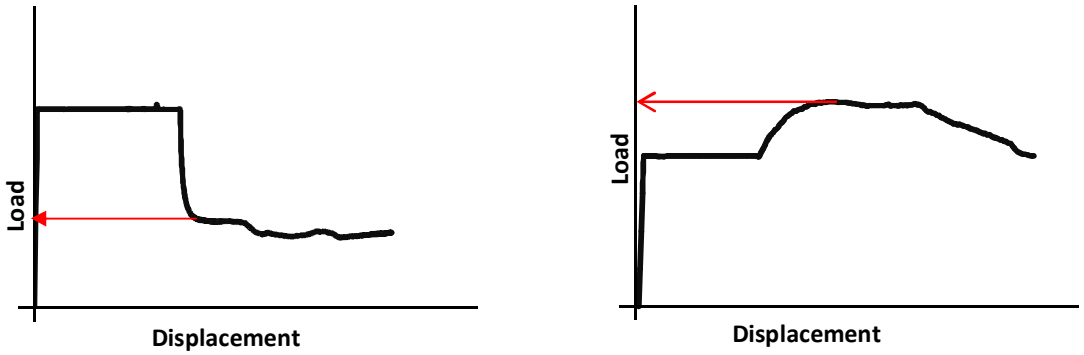

a) *b)*

Figure 4.1.4.1. a) load-displacement curve of models where concrete failure happens during heating, in phase 2; b) load-displacement curve of models where concrete failure happens after heating, in phase 3.

Anchor	Preloading	Condition	Fire duration /min	Edge distance *c*/mm	Embedment depth h_{ef}/mm	Stud diameter *d*/mm	Peak load *Vu*/kN	Horizontal displacement /mm
c75h75d16	/	Hot state	15	75	75	16	8.921,2	1,97
			60	75	75	16	6.748,6	1,91
		Cold state	15	75	75	16	10.171,8	4,12
			60	75	75	16	4.261,8	7,90
	Preloading V=12,63 kN	Hot state	15	75	75	16	13.121,4	2,82
			60	75	75	16	3.887,8	18,30
		Cold state	15	75	75	16	6.293,6	4,60
			60	75	75	16	1.309,4	40,40
c75h75d25	/	Hot state	15	75	75	25	10.409,2	2,94
			60	75	75	25	5.322,6	6,07
		Cold state	15	75	75	25	12.163,4	5,28
			60	75	75	25	7.066,6	1,89
	Preloading V=13,60 kN	Hot state	15	75	75	25	9.741,2	1,85
			60	75	75	25	2.263,6	15,60
		Cold state	15	75	75	25	11.293,0	5,53
			60	75	75	25	1.152,5	37,20
c100h75d25	/	Hot state	15	100	75	25	13.823,0	1,02
			60	100	75	25	6.259,0	3,19
		Cold state	15	100	75	25	17.021,2	0,45
			60	100	75	25	8.729,6	1,42
	Preloading V=19,67 kN	Hot state	15	100	75	25	11.101,0	1,27
			60	100	75	25	2.460,0	19,06
		Cold state	15	100	75	25	7.348,8	4,78
			60	100	75	25	1.205,1	44,20
c150h75d25	/	Hot state	15	150	75	25	15.966,6	0,91
			60	150	75	25	6.767,6	5,02
		Cold state	15	150	75	25	30.494,0	0,44
			60	150	75	25	8.382,2	5,87
	Preloading V=33,48 kN	Hot state	15	150	75	25	10.480,8	2,15
			60	150	75	25	916,3	117,26
		Cold state	15	150	75	25	2.970,8	22,50
			60	150	75	25	589,5	286,81

Figure 4.1.4.2 Peak loads for tested models with 15 and 60 min fire duration (c75h75d16; c75h75d25; c100h75d25; c150h75d25)

Anchor	Preloading	Condition	Fire duration /min	Edge distance *c*/mm	Embedment depth h_{ef}/mm	Stud diameter *d*/mm	Peak load *Vu* /kN	Horizontal displacement /mm
c75h95d25	/	Hot state	15	75	95	25	10.174,4	2,55
			30	75	95	25	7.439,2	3,92
			60	75	95	25	4.564,2	11,40
		Cold state	15	75	95	25	14.139,6	3,33
			30	75	95	25	13.300,4	2,89
			60	75	95	25	4.640,6	3,99
	Preloading V=14,43 kN	Hot state	15	75	95	25	9.974,6	2,95
			30	75	95	25	3.846,8	7,20
			60	75	95	25	2.199,8	18,17
		Cold state	15	75	95	25	3.649,4	9,20
			30	75	95	25	2.082,0	15,76
			60	75	95	25	958,4	37,70
c100h95d25	/	Hot state	15	100	95	25	14.580,2	2,59
			30	100	95	25	10.054,0	4,08
			60	100	95	25	6.541,0	10,60
		Cold state	15	100	95	25	18.253,0	0,53
			30	100	95	25	17.758,0	0,52
			60	100	95	25	7.962,4	4,95
	Preloading V=20,74 kN	Hot state	15	100	95	25	13.166,0	2,84
			30	100	95	25	8.306,8	6,04
			60	100	95	25	3.948,6	18,60
		Cold state	15	100	95	25	6.281,2	4,87
			30	100	95	25	2.779,8	15,90
			60	100	95	25	1.234,5	41,20
c150h95d25	/	Hot state	15	150	95	25	18.374,8	2,93
			30	150	95	25	12.953,8	4,98
			60	150	95	25	9.108,8	11,45
		Cold state	15	150	95	25	34.400,0	0,62
			30	150	95	25	34.752,0	0,95
			60	150	95	25	11.549,8	6,30
	Preloading V=35,02 kN	Hot state	15	150	95	25	16.751,6	3,60
			30	150	95	25	6.557,8	9,60
			60	150	95	25	3.273,0	34,00
		Cold state	15	150	95	25	4.560,4	10,30
			30	150	95	25	2.129,2	34,90
			60	150	95	25	1.021,5	92,50

Figure 4.1.4.3 Peak loads for tested models with 15, 30 and 60 min fire duration (c75h95d25; c100h95d25; c150h95d25)

4.1.5 Typical failure mode

Figure 4.1.5.1 shows the numerical crack patterns for model c75h75d25 in the step where peak load has occured, loaded towards the free edge after fire exposure. After 15 min of fire, the fracture in the cold state loading initiates at the upper side of the shaft. After longer fire durations, cracks from the upper side of the shaft and the crack on the back of the head appear almost at the same time, unlike their propagation after 15 minute fire duration where the crack on the upper side of the shaft appeares first. For cracks in the hot state, it can be seen that they are basically developing at the same time. Damage of concrete in the cold state is lower than in the hot state. Later will be shown that the resistance of the concrete in the cold state is higher than in the hot state for models without preloading.

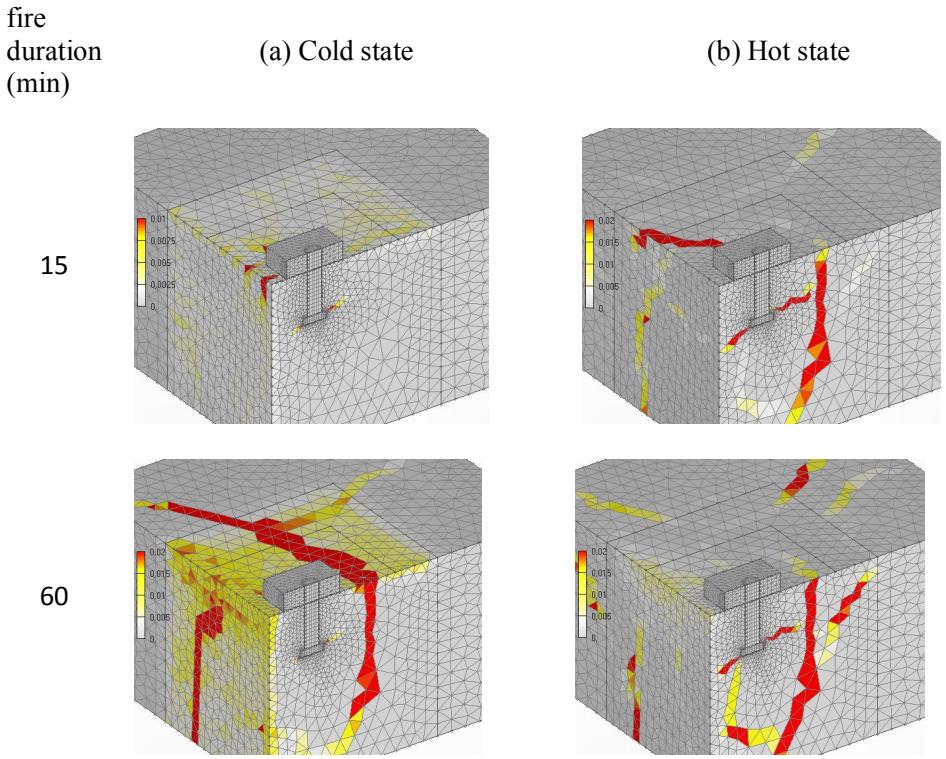

Figure 4.1.5.1 Numerical fracture patterns of anchor c75h75d25 loaded in shear in concrete C20/25 after different fire durations. (a) Cold state; (b) Hot state. Loading direction: towards free edge

4.2 Comparison and discussion

4.2.1 Comparison between preloaded and not preloaded anchors

Figure 4.2.1.1 shows the resistance comparison between anchors with and without preloading in the hot state as a function of temperature duration for anchors with diameter d=25mm and embedment depth h_{ef}=95mm for three different edge distances (i.e. c75h95d25, c100h95d25 and c150h95d25).

It can be seen that in the case of 15 min fire exposure, preloading does not make big difference in load capacity for small edge distances (c_1=75mm) where the resistance reduces by around 2% due to preloading. For large edge distances (c_1=150 mm) and 15 min fire exposure, the resistance of the anchorages against concrete edge failure reduces by around 50% due to preloading. Preloading before 30 min fire exposure cause 45% reduction for small edge distances and 60% reduction for large edge distances. With prolonged fire duration, the peak loads are gradually unifying.

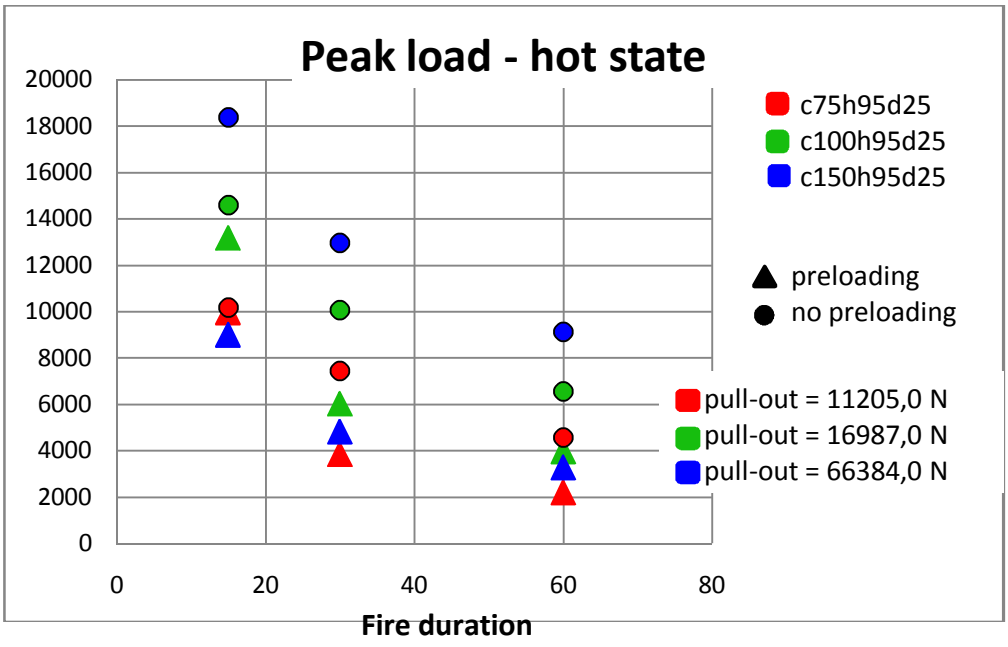

Figure 4.2.1.1 Comparison between results of preloaded and not preloaded models in hot state with respect to different fire duration (15 min, 30 min, 60 min, 90 min) and edge distance (75 min, 100 min, 150 mm)

Cold state shows a larger load capacity reduction due to preloading. Cases with 15 and 30 min fire exposure show that the resistance of the anchorages against concrete edge failure reduces by around 70% for small edge distances (c_1=75 mm) and 85% for large edge distances (c_1=150 mm). It is worth noting that the resistances of preloaded anchors in the cold state appear to be very similar, regardless of the distance between anchor and the edge of concrete. Also, with increasing fire duration, the differences in resistance of preloaded anchors in cold state are much smaller than those of not preloaded anchors.

Bearing capacity for not preloaded anchors is higher in the cold state then in the hot state. In contrary to the not preloaded anchors, preloaded anchors show lower resistances in cold state than in the hot state. Because of that, the cold state resistance is relevant for preloaded anchors.

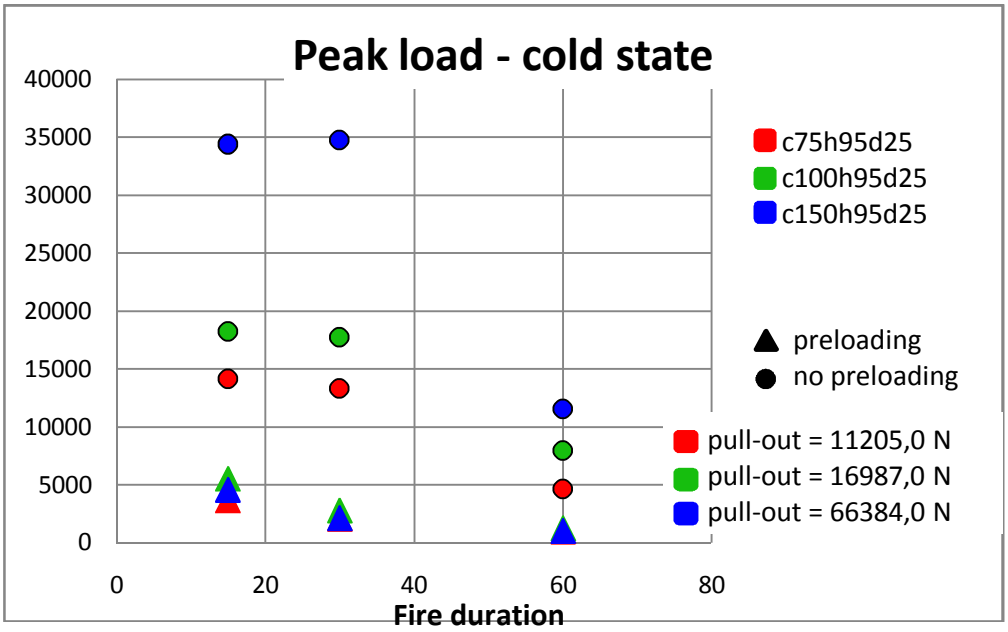

Figure 4.2.1.2 Comparison between results of preloaded and not preloaded models in cold state with respect to different fire duration (15 min, 30 min, 60 min, 90 min) and edge distance (75 mm, 100 mm, 150 mm)

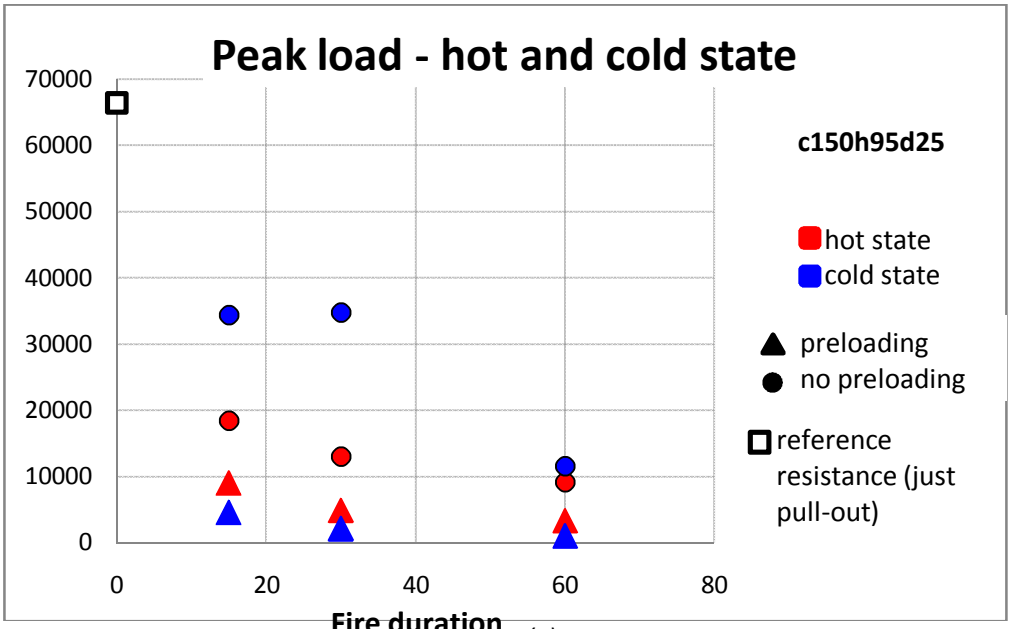
Peak load - hot and cold state
70000
60000
50000
40000
30000
20000
10000
0
0
20
40
60
80
Fire duration
c150h95d25
hot state
cold state
preloading
no preloading
reference resistance (just pull-out)

(a)

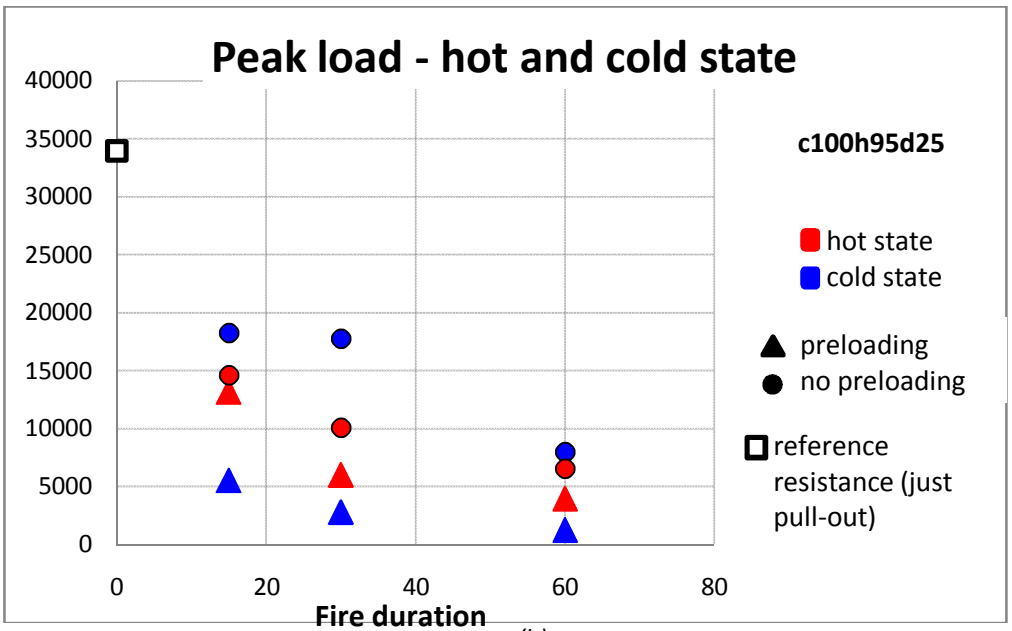
Peak load - hot and cold state
40000
35000
30000
25000
20000
15000
10000
5000
0
0
20
40
60
80
Fire duration
c100h95d25
hot state
cold state
preloading
no preloading
reference resistance (just pull-out)

(b)

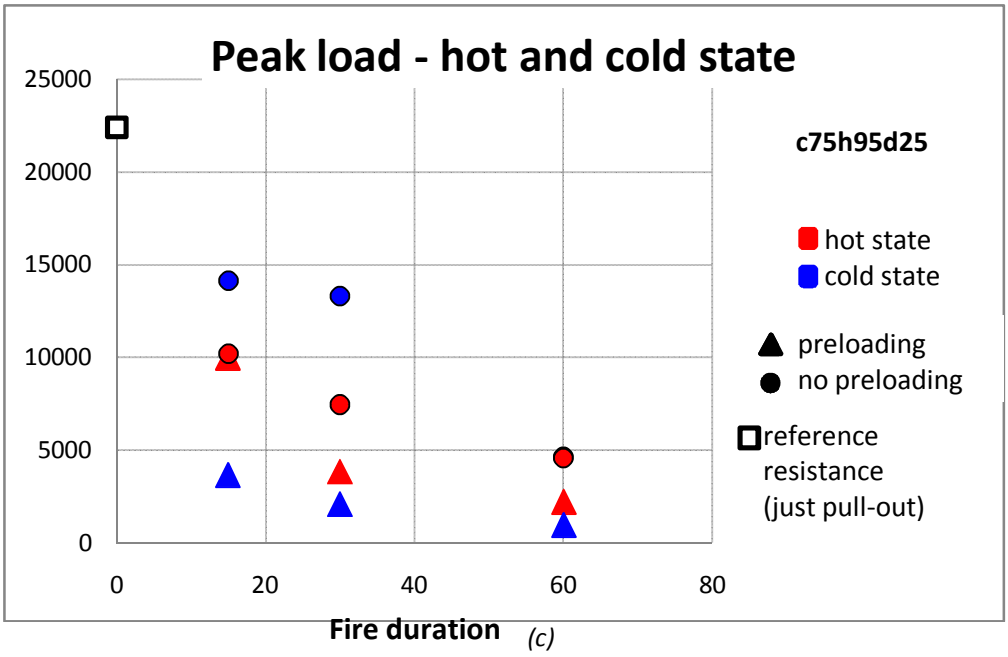

(c)

Figure 4.2.1.3 Comparison between hot and cold state of phases with preloading and without preloading with respect to different fire duration (15 min, 30 min, 60 min, 90 min) for models: (a) c150h95d25 (b) c100h95d25 (c) c75h95d25

As stated earlier, carring capacity for preloaded anchors is higher in the hot state then in the cold state. Therefore, more attention should be devoted to the cold state resistance. Due to the cooling process the confinement stresses are released. Because of the inhomogeneity of the temperature field (e.g. surface of the concrete cools faster than the concrete inside the slab), through the cooling process additional damage of concrete can be generated.

In cold state the resistance of preloaded anchors, compared to the reference resistance,is strongly reduced for all edge distancesand for all durations of fire. For anchors placed closer the edge (c_1=75mm) only 13 % of the reference resistance remained after 15 min of fire, 9% after 30 min of fire and 4 % after 60 min of fire. Anchors with greater edge distances show similar reduction for cold state after 15 min fire exposure, but after longer fire durations the reduction of reference resistance is getting bigger.

In the hot state, after 15 min of fire exposure, the load carrying capacities of not preloaded anchors exposed to fire were reduced to 30% (c_1 = 150 mm) and 45% (c_1 = 75 mm and 100 mm) of the corresponding reference resistances at ambient temperature. After 30 min of fire exposure, the resistance is 20%(c_1 = 150 mm) and 30 % (c_1 = 75 mm) of referent resistance. The greater reduction for preloaded anchors is evident after 60 min fire exposure where the concrete is so damaged that it has insignificant bearing capacity, in cold and hot state.

HOT STATE

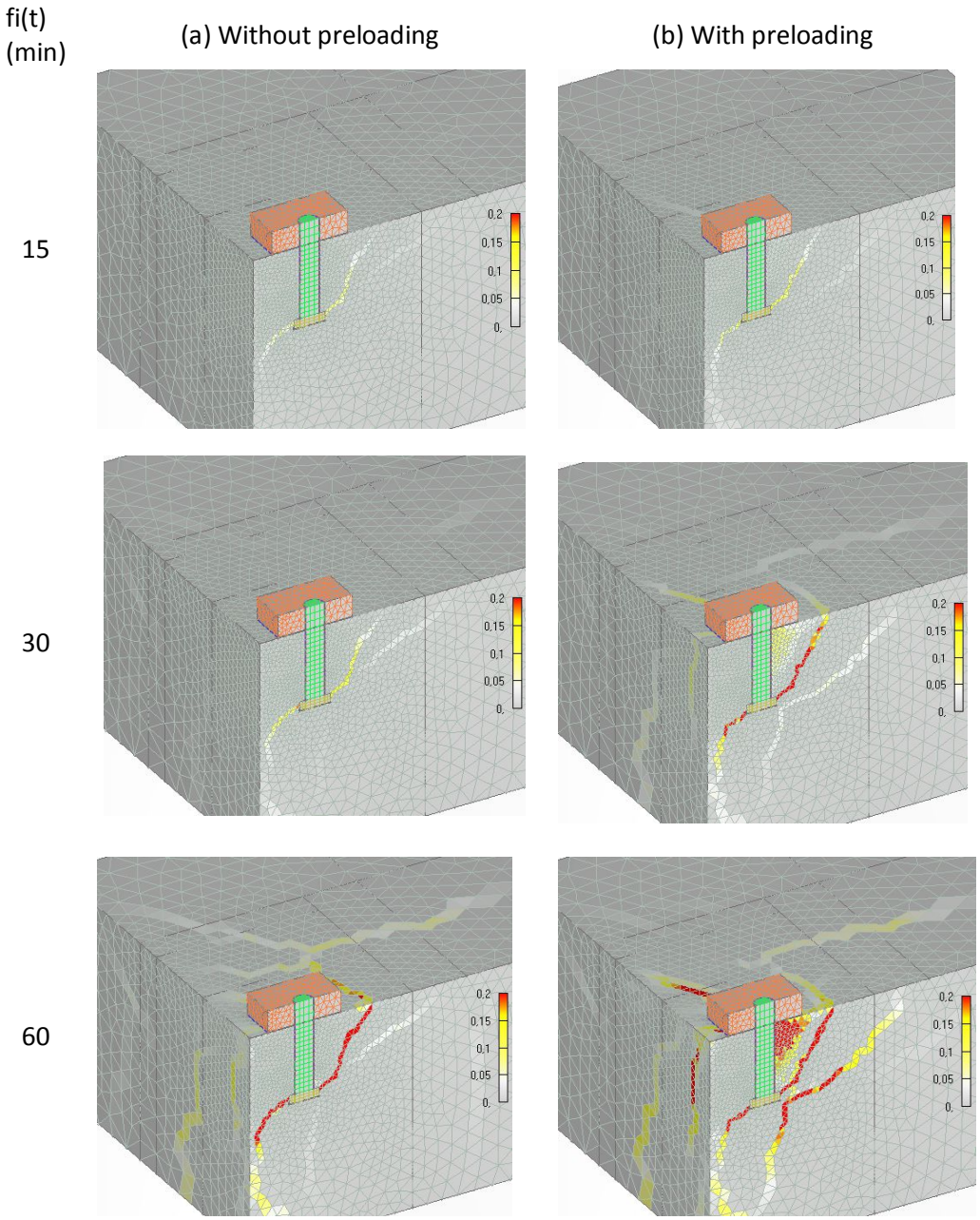

Figure 4.2.1.4 Numerical fracture patterns of anchor c75h95d25 loaded in shear in concrete C20/25 after different fire durations. (a) Not preloaded model; (b) Preloaded model. Loading direction: towards free edge; Temperature condition: hot state.

COLD STATE

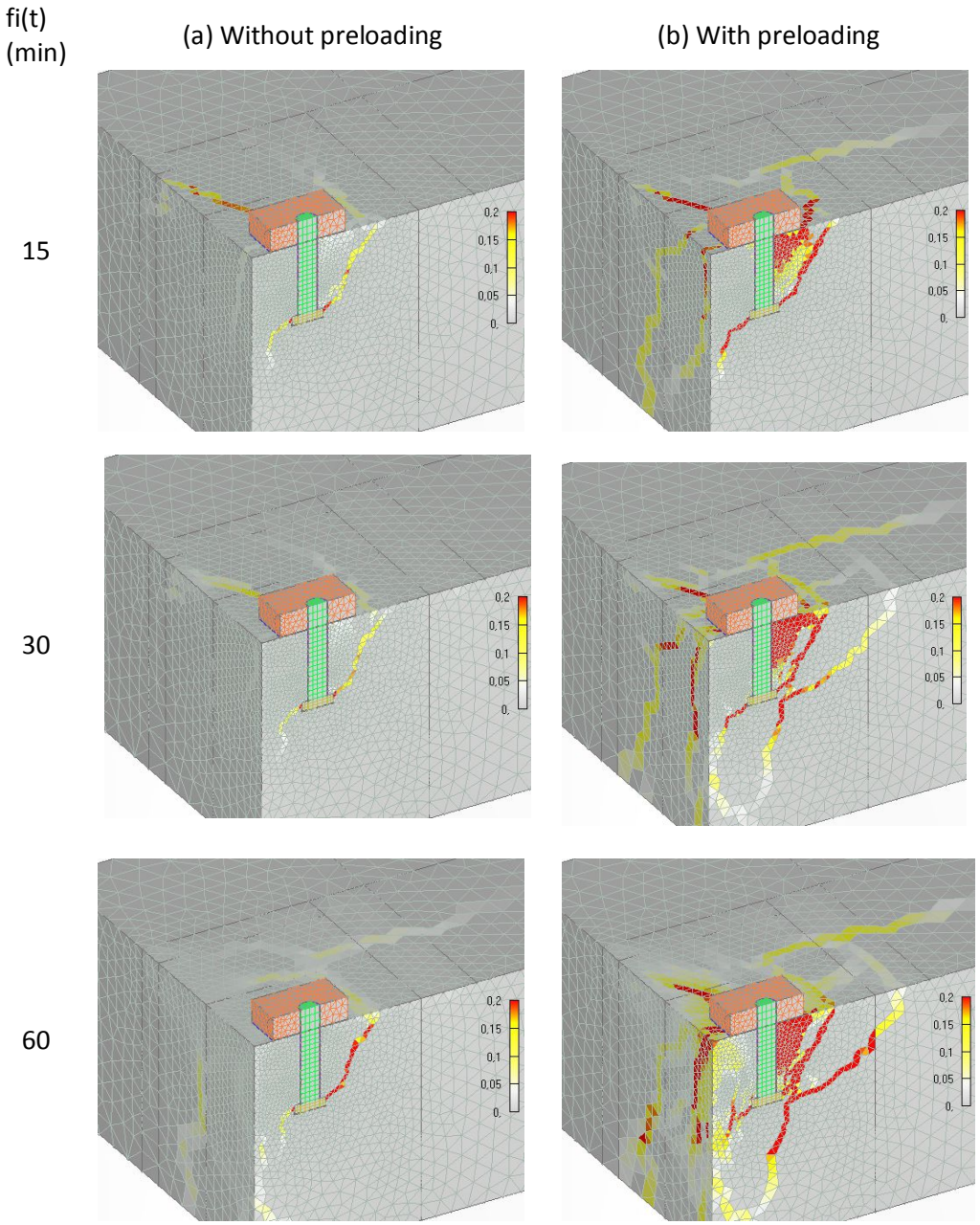

Figure 4.2.1.5 Numerical fracture patterns of anchor c75h95d25 loaded in shear in concrete C20/25 after different fire durations. (a) Not preloaded model; (b) Preloaded model. Loading direction: towards free edge; Temperature condition: cold state.

From the images shown above it can be seen that tested models with preloaded anchors have significantly greater damage of concrete than those with not preloaded anchors. Damage of concrete is greater in cold state for preloaded anchors and in hot state for not preloaded anchors.

4.2.2 Comparison of different embedment depths

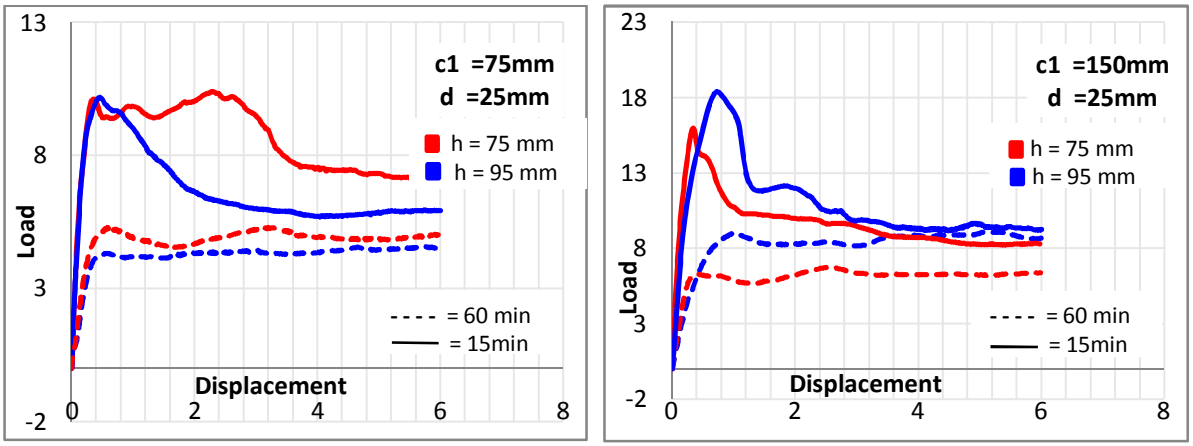

(a) *(b)*

Figure 4.2.2.1 Load-displacement curves for hot state of models with different embedment depth h=75mm; h=95mm (a) c_1=75mm; d=25mm; (b) c_1=150mm; d=25mm, after 15 min and 60 min of fire exposure

For anchors located at a bigger distance from the concrete edge (c_1=150 mm), the embedment depth has a greater impact on capacity of anchors loaded in shear. When the anchor is located close to an edge (c_1=75 mm), embedment depth does not have much influence in bearing capacity, which is reasonable due to the penetration of heat into concrete member from both sides of the edge.With decreasing embedment depth, resistance of concrete loaded in shear decreases. Reduction is up to 15 % for 15 min fire duration and 25 % for 60 min fire duration for models with anchors set 150 mm from the edge.

The greater the thermal damage in concrete is, the greater is the influence of the embedment depth on the concrete edge failure resistance. This could be explained by considering the fact that the concrete further away from the edge suffers less thermal damage. Therefore, the resistance of anchors with larger embedment depth is higher.

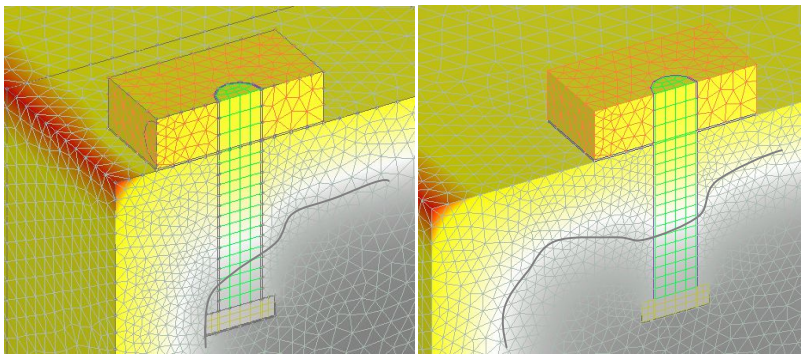

(a) *(b)*

Figure 4.2.2.2 Temperature distribution of anchors embedded in concrete C20/25 exposed to fire on both sides of the edge. (a) Edge distance c_1 = 75 mm; (b) Edge distance c_1 = 150 mm;

4.2.3 Comparison of different edge distances

Figure 4.2.3.1 shows the comparison between the load-displacement curves for models with different edge distanc. Models with larger edge distance show bigger resistance of the anchorages against concrete edge failure. For 15 min fire exposure, with decreasing edge distance from 150 mm to 75 mm, bearing capacity reduces by around 40 %. The same reduction for 60 min of fire is 25%.The load capacity of anchors exposed to 15 fire is 55% higher than thoseexposed to 60min of fire. As expected, with increase of edge distance the load-bearing response is much stiffer, i.e. the peak load is reached at lower displacement.

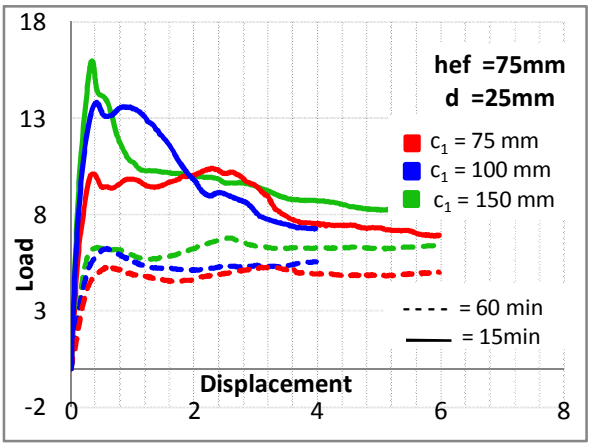

Figure 4.2.3.1 Load-displacement curves of models with different edge distance(c_1=75mm; c_1=100mm; c_1=150mm) after 15 min and 60 min fire exposure; h_{ef}=75mm; d=25mm.

Temperature distribution around anchor

Figure 4.2.3.2 shows typical temperature distribution in the model with the anchor edge distance of 75 mm, 100 mm and 150 mm after exposing to fire. For anchors with the same embedment depth, the temperature field around the anchor is mainly affected by the edge distance, due to the heating from the front face. In the case with the edge distance of 75 mm, the temperature penetration reaches the anchor head after 30 min of fire exposure, whereas the same tamperature distribution for the case with the edge distance of 150 mm occurs only after 60 min of fire. This will result in a much higher resistance for anchor with larger edge distance.

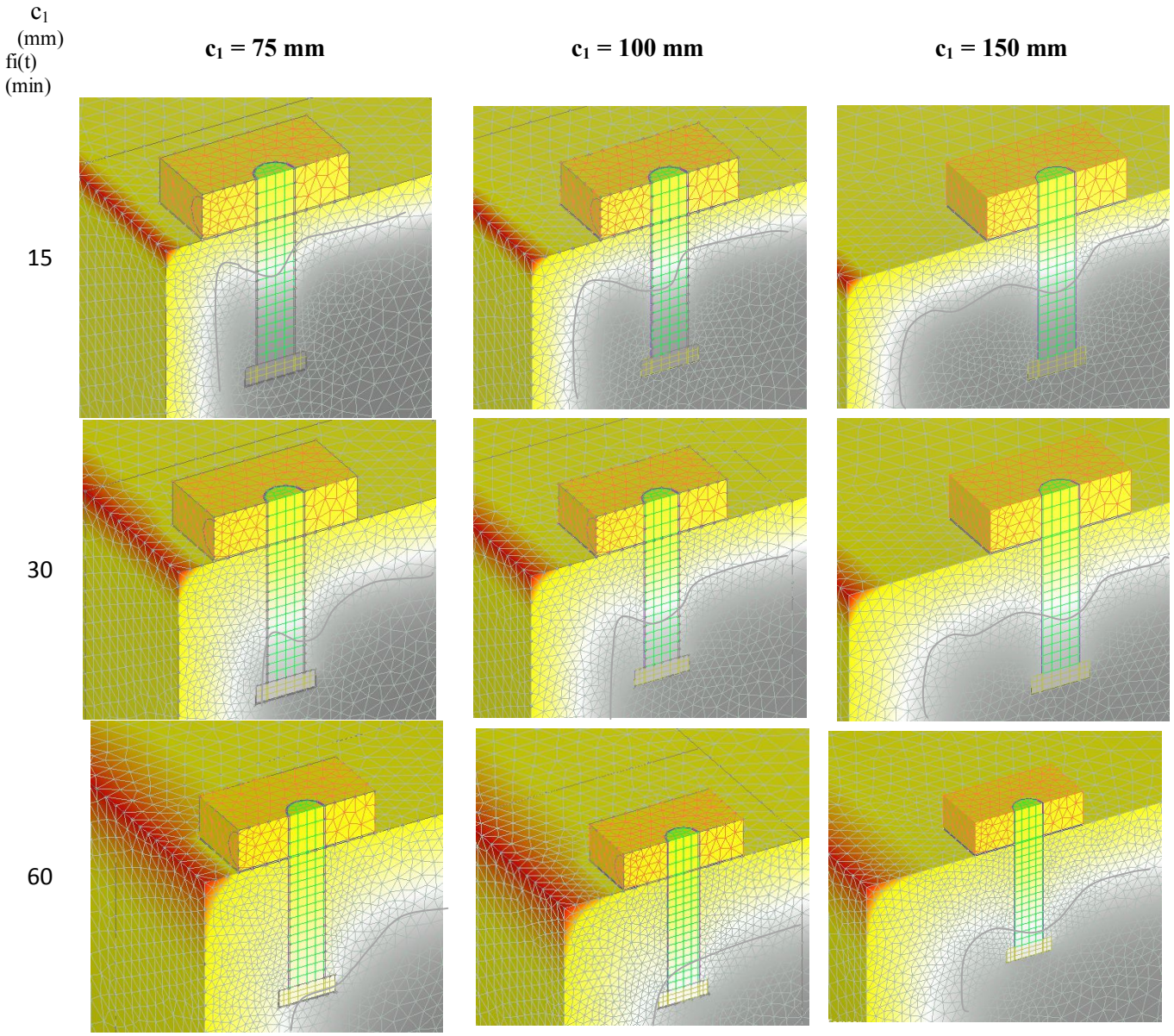

Figure 4.2.3.2 Numerical temperature distribution of anchors embedded in concrete C20/25 exposed to fire on both sides of the edge. (a) Edge distance c_1 = 75 mm; (b) Edge distance c_1 = 100 mm; (c) Edge distance c_1 = 150 mm

4.2.4 Comparison of different anchor diameter

It can be seen that resistance of anchorages against concrete edge failure after 15 min of fire exposure increases with increasing diameter of an anchor. The anchors with smaller diameter behave stiffer than the anchor with larger diameter, i.e. the peak load is reached at lower displacement. The results for 60 min fire are unexpected because the resistence of model with 16 mm anchor diameter is higher then the resistance of anchor with 25 mm diameter. This may be due to small edge distance as the temperature reaches anchor with larger diameter sooner. For larger edge distances, the situation is probably different and the anchor with larger diameter has higher resistance, no matter how long the model was exposed to fire.

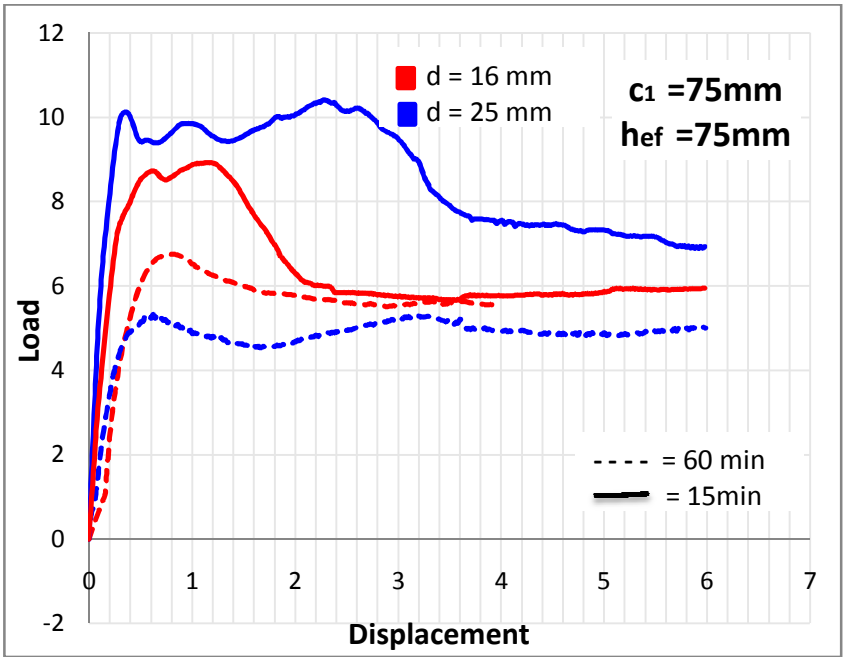

Figure 4.2.4.1 Load-displacement curves of hot state for models with different anchor diameter (d=16 mm; d=25 mm) after 15 min and 60 min of fire exposure; c_1=25 mm; h_{ef}=75 mm

4.2.5 Experimental results

To verify the numerical prediction, the numerical results are compared with experimental ones (K.Tian, 2018). Figure 4.2.5.1 shows the comparison between the numerical and experimental load-displacement curves in cold state after 15 and 60 min fire exposure. The load-displacement curves for anchors with different edge distance are shown. It can be seen that the numerical curves predict stiffer response than the experimental curves, especially for the anchor with large edge distance. As stated previously, this can be attributed to the local damage of concrete, which cannot be accounted for in the macroscopic finite element analysis. Nevertheless, the peak loads are very well predicted.[1]

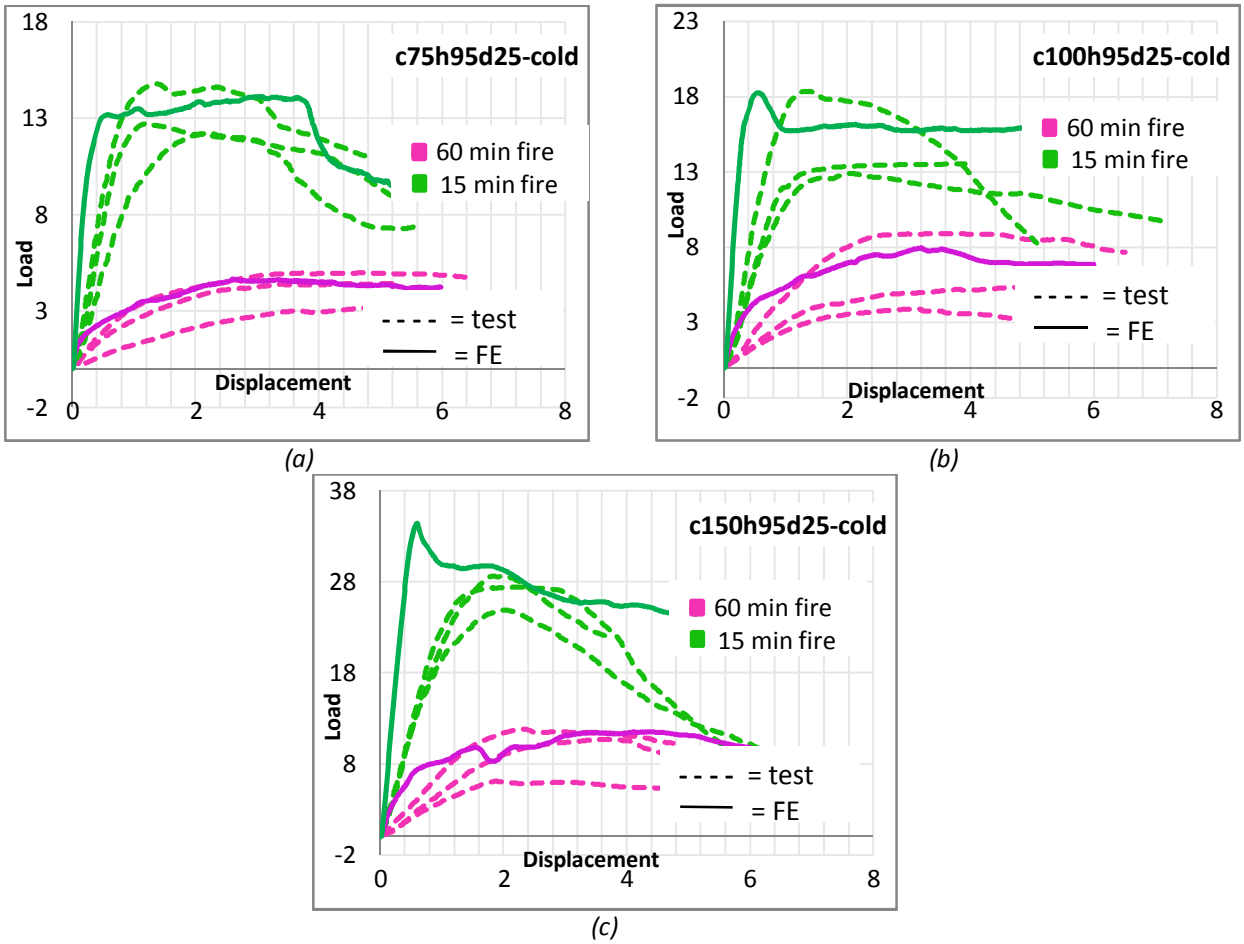

Figure 4.2.5.1 Comparison between numerical and experimental load-displacement curves after 15 min and 60 min of fire exposure in concrete grade C20/25. (a) c75h95d25; (b) c100h95d25; (c) c150h95d25

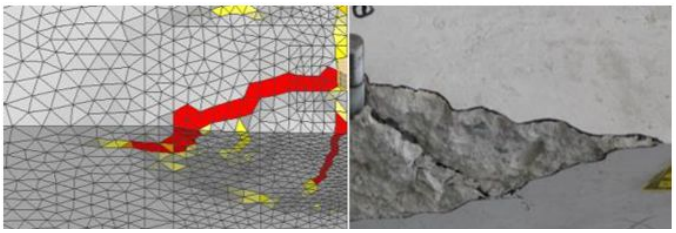

Figure 4.2.5.2 Predicted and observed failure modes (ambient temperature).[1]

5. CONCLUSIONS

(1) The main aim of the research presented in the paper was to investigate the difference in concrete edge failure of anchors with and without preloading in shear. Preloading of anchors lead to significant reduction in resistance after fire exposure compared to the anchors without preloading. For preloaded anchors resistance is higher in the hot state than in the cold state, unlike anchors without preloading where the resistance is higher in cold state.

(2)The anchor diameter governs the shear stiffness of the anchor at ambient temperature[1]; however, after exposure to fire the edge distance become the dominant factors. The diameter and embedment depth do not influence the shear stiffness significantly after exposure to fire. With increasing fire duration, the shear stiffness is reduced remarkably.

(3) On the basis of this work, it is worth focusing on the shear resistance of preloaded anchors regarding concrete edge failure in the cold state.

(4) The results of the study indicate that preloading makes a significant reduction of resistance and the cold state resistance is relevant for concrete edge failure of preloaded anchors close to free edge. Therefore, it would be possible that the failure of steel could be critical in the hot state.

6. BIBLIOGRAPHY

[1] Kaipei Tian (2018) Experimental study on concrete edge failure of single headed stud anchors after fire exposure.

[2] Eligehausen, R., Mallée, R., Silva, J.F. (2006) Anchorage in concrete construction. Berlin: Ernst & Sohn.

[3] Ožbolt, J., Li, Y., Kožar, I. (2001) Microplane model for concrete with relaxed kinematic constraint. International Journal of Solids and Structures. 38(16), 2683–2711.

[4] Ožbolt, J. (1998) MASA-macroscopic space analysis, Internal Report. Institute of Construction Materials, University of Stuttgart, Germany.

[5] European Committee for Standardization (2003) Eurocode 1 1991-1-2: Actions on structures - Part 1-2: General actions - Actions on structures exposed to fire.

[6] Bošnjak, J. (2014) Explosive spalling and permeability of high performance concrete under fire – numerical and experimental investigations. University of Stuttgart.